THE JOURNAL OF BIOLOGICAL CHEMISTRY VOL. 291, NO. 36, pp. 18700–18717, September 2, 2016

Functional Consequences of Mannose and Asialoglycoprotein Receptor Ablation*[S]

Received for publication, May 19, 2016, and in revised form, July 11, 2016 Published, JBC Papers in Press, July 12, 2016, DOI 10.1074/jbc.M116.738948

Yiling Mi, Marcy Coonce, Dorothy Fiete, Lindsay Steirer, Gabriela Dveksler, R. Reid Townsend, and Jacques U. Baenziger[1]

From the Department of Biochemistry and Molecular Biophysics, Washington University School of Medicine, St. Louis, Missouri 63110

The mannose receptor (ManR, Mrc1) and asialoglycoprotein receptor (ASGR, Asgr1 and Asgr2) are highly abundant endocytic receptors expressed by sinusoidal endothelial cells and parenchymal cells in the liver, respectively. We genetically manipulated either receptor individually or in combination, revealing phenotypic changes in female and male mice associated with changes in circulating levels of many glycoproteins. Both receptors rise and fall in response to progesterone during pregnancy. Thirty percent of *Asgr2*$^{-/-}$ and 65% of Mrc*1*$^{-/-}$ *Asgr2*$^{-/-}$ mice are unable to initiate parturition at the end of pregnancy, whereas *Mrc1*$^{-/-}$ mice initiate normally. Twenty five percent of Mrc*1*$^{-/-}$*Asgr2*$^{-/-}$ male mice develop priapism when mating due to thrombosis of the penile vein, but neither *Mrc1*$^{-/-}$ nor *Asgr2*$^{-/-}$ mice do so. The half-life for luteinizing hormone (LH) clearance increases in *Mrc1*$^{-/-}$ and *Mrc1*$^{-/-}$ *Asgr2*$^{-/-}$ mice but not in *Asgr2*$^{-/-}$ mice; however, LH and testosterone are elevated in all three knockouts. The ManR clears LH thus regulating testosterone production, whereas the ASGR appears to mediate clearance of an unidentified glycoprotein that increases LH levels. More than 40 circulating glycoproteins are elevated >3.0-fold in pregnant *Mrc1*$^{-/-}$*Asgr2*$^{-/-}$ mice. Pregnancy-specific glycoprotein 23, undetectable in WT mice (<50 ng/ml plasma), reaches levels of 1–10 mg/ml in the plasma of *Mrc1*$^{-/-}$*Asgr2*$^{-/-}$ and *Asgr2*$^{-/-}$ mice, indicating it is cleared by the ASGR. Elevation of multiple coagulation factors in *Mrc1*$^{-/-}$*Asgr2*$^{-/-}$ mice may account for priapism seen in males. These male and female phenotypic changes underscore the key roles of the ManR and ASGR in controlling circulating levels of numerous glycoproteins critical for regulating reproductive hormones and blood coagulation.

The asialoglycoprotein receptor (ASGR),[2] consisting of two subunits designated Asgr1 and Asgr2, and the mannose receptor (ManR), consisting of a single subunit designated Mrc1, are highly abundant, glycan-specific, endocytic receptors that are expressed by parenchymal cells (PC) and sinusoidal endothelial cells (SEC) in the liver, respectively (1–6). The ASGR was first identified by Ashwell and co-workers (7) on the basis of its ability to rapidly remove glycoproteins bearing *N*-linked glycans terminating with the structure Galβ1,4GlcNAc (Fig. 1) from the blood. Exogenous glycoproteins bearing glycans terminating with the structure GalNAcβ1,4GlcNAc, Galβ1,4[Fucβ1,3]GlcNAc (denoted Lewis^X), or in some species the structure Siaα2,6GalNAcβ1,4GlcNAc are also recognized by the ASGR and rapidly cleared (9–11). PCs express 500,000 ASGR sites at their plasma membrane that are rapidly internalized and replaced by recycling receptors (12). Mice that have had either the *Asgr1* or *Asgr2* subunit ablated do not exhibit ASGR binding activity at the plasma membrane, yet apparently they do not display major increases in circulating glycoproteins bearing glycans that should be recognized by the ASGR and do not exhibit an evident phenotype (13–15). Physiological challenges have been used to reveal functional deficiencies in *Asgr1*$^{-/-}$ and *Asgr2*$^{-/-}$. For example, Marth and co-workers (16) have shown that *Asgr1*$^{-/-}$ and *Asgr2*$^{-/-}$ mice exhibit increased resistance to developing disseminated intravascular coagulation during pneumococcal sepsis induced with increasing doses of bacteria. Similarly, platelets subjected to cold storage, which exposes terminal galactose at their surface, are cleared more slowly when introduced into *Asgr1*$^{-/-}$ and *Asgr2*$^{-/-}$ mice than WT mice. Thus, the ASGR may also play a role in platelet clearance under physiological circumstances (17).

The ManR was identified in macrophages and SECs in the liver on the basis of its ability to clear glycoproteins bearing oligomannose-type glycans (Fig. 1) from the blood (18). SECs express 500,000 ManR-binding sites at their plasma membrane that are rapidly internalized along with any bound ligand (2). Important roles in innate immunity and clearance of glycoproteins from the blood have been attributed to the ManR based on its ability to bind glycans on pathogens and glycoproteins such as lysosomal enzymes (19, 20). Lee *et al.* (21) reported that *Mrc1*$^{-/-}$ mice have elevated circulating levels of 52 unique proteins, including lysosomal enzymes and procollagen fragments,

* This work was supported by National Institutes of Health Grants R01-CA21923 and R01-HD058474 (to J. U. B.), Washington University Institute of Clinical and Translational Sciences Grant UL1 TR000448 from the National Center for Advancing Translational Sciences, and National Institutes of Health Grant P41 GM103422-35 from NIGMS. The authors declare that they have no conflicts of interest with the contents of this article. The content is solely the responsibility of the authors and does not necessarily represent the official views of the National Institutes of Health.

[S] This article contains supplemental Table SI.

[1] To whom correspondence should be addressed: Dept. of Biochemistry and Molecular Biophysics, Washington University School of Medicine, 660 South Euclid Ave., St. Louis, MO 63110. E-mail: Baenziger@wustl.edu.

[2] The abbreviations used are: ASGR, asialoglycoprotein receptor; ManR, macrophage mannose receptor; PC, hepatic parenchymal cells; SEC, sinusoidal endothelial cells; LH, luteinizing hormone; TSH, thyroid stimulating hormone; StAR, steroidogenic acute regulatory protein; 20αHSD, 20α-hydroxysteroid dehydrogenase; PSG, pregnancy-specific glycoprotein; d.p.c., day post-coitum; vWF, von Willebrand factor; TGFBIp/β Ig-h3, transforming growth factor β_1-induced protein ig-h3; BisTris, 2-[bis(2-hydroxyethyl)amino]-2-(hydroxymethyl)propane-1,3-diol; MAF, multiaffinity fractionation; WFA, *W. floribunda* agglutinin; RCA$_I$, *R. communis* agglutinin-I.

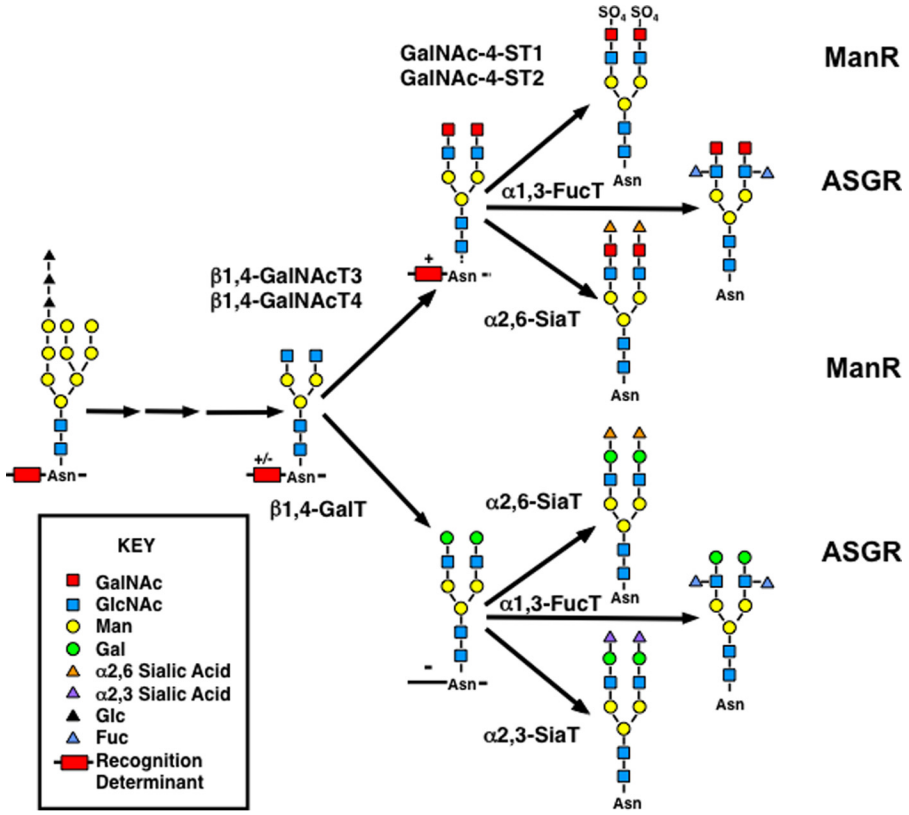

FIGURE 1. **Synthetic pathways producing *N*-linked glycans recognized by the mannose and asialoglycoprotein receptors.** A glycan containing three Glc, nine Man, and two GlcNAc residues is transferred cotranslationally from dolichol-pyrophosphate to Asn-Xaa-(Ser/Thr) acceptor sequences on proteins in the endoplasmic reticulum. Removal of outer Glc and Man residues and addition of GlcNAc residues produce a structure with two terminal GlcNAc residues. Glycans on glycoproteins that contain a peptide recognition determinant that is recognized by either β1,4-GalNAcT3 or β1,4-GalNAcT4 and are expressed in cells containing one or both transferases will be modified with β1,4-GalNAc. The resulting structure can be further modified with SO_4 linked to the 4-hydroxyl of the GalNAc, Fuc linked to the 3-hydroxyl of the underlying GlcNAc, or Sia linked to the 6-hydroxyl of the GalNAc. In the absence of the recognition determinant or either β1,4-GalNAcT3 or β1,4-GalNAcT4, the *N*-linked glycans with terminal GlcNAc are modified with β1,4-linked Gal. The terminal Gal can be modified with either α1,3- or α1,6-linked Sia or with underlying GlcNAc can be modified with α1,3-linked Fuc. Glycans containing Man or GlcNAc are recognized by the ManR. Glycans containing terminal GalNAc-4-SO_4 are recognized by a distinct region of the ManR, the Cys-rich or R-type lectin domain. Glycans containing terminal β1,4-linked Gal or GalNAc are recognized by the ASGR in the presence or absence of α1,3-linked Fuc on the underlying GlcNAc. In mice the presence of Sia or SO_4 on the terminal GalNAc or Gal prevents recognition by the ASGR.

clearly establishing a role for the ManR in clearance of glycoproteins bearing oligomannose-type glycans. Nonetheless, *Mrc1*$^{-/-}$ mice did not manifest an obvious phenotype.

In earlier studies, we demonstrated that glycoproteins such as luteinizing hormone (LH) bearing *N*-linked glycans terminating with SO_4-4-GalNAcβ1,4GlcNAc (Fig. 1) are cleared from the blood by a dimeric form of the same ManR expressed in SECs found in the liver (1, 22–24). Terminal GalNAc-4-SO_4 is bound by a distinct region of the ManR (Mrc1), denoted as the cysteine-rich or R-type lectin domain located at the N terminus, whereas glycans containing terminal mannose are bound by C-type lectin domains located near the transmembrane domain (25–28). The sulfotransferase GalNAc-4-sulfotransferase-1 (GalNAc-4-ST1, CHST8) mediates the addition of SO_4 to *N*-linked glycans terminating with GalNAcβ1,4GlcNAc (Fig. 1) on LH (29–31), generating ligands that are recognized by the ManR. We determined that *N*-linked glycans on LH produced by *GalNAc-4-ST1*$^{-/-}$ mice terminated with Siaα2,6GalNAcβ1,4GlcNAc instead of SO_4-4-GalNAcβ1,4GlcNAc (Fig. 1). As a consequence, LH levels were elevated because LH was no longer cleared by the ManR, resulting in higher levels of testosterone and estrogen in males and females, respectively (32). In these sulfotransferase knock-out mice, males underwent precocious sexual development and had enlarged seminal vesicles due to the elevated testosterone. Female mice also underwent precocious sexual development, had enlarged and highly vascularized uteri, and were constantly in estrus due to the elevated estrogen levels. The phenotype of the *GalNAc-4-ST1*$^{-/-}$ mice supported our hypothesis that the episodic rise and fall of LH levels critical for maximal stimulation of the LH receptor in the testis and ovary depend not only on regulated release of LH-containing granules by the pituitary but also on rapid clearance of the released LH by the ManR (Mrc1). Because the K_d value of the ManR for binding LH glycans is well above the maximal levels of LH that are attained in the blood, the half-life for clearance of LH by the ManR should remain constant regardless of the concentration of LH in the blood. However, the clearance rate should be determined by the amount of ManR expressed.

We recently reported that expression of both the ASGR and the ManR increased in the liver of pregnant mice in response to progesterone. We demonstrated that levels of receptor expression determined the rate of clearance from the blood of glycoproteins bearing glycans recognized by each receptor (9). As a key exemplar ligand, we generated recombinant pregnancy-specific glycoprotein 23 (PSG23), a member of the murine PSG

sub-family within the greater carcinoembryonic antigen protein family (33, 34), bearing seven *N*-linked glycans each terminating with GalNAc-4-SO_4. Clearance of this form of recombinant PSG23 was abolished in *Mrc1*$^{-/-}$ mice, consistent with the proposed role of the ManR in LH clearance (9).

Whereas *Mrc1*$^{-/-}$ and *Asgr2*$^{-/-}$ mice were fertile, the pattern of ASGR and ManR expression suggested that one or both receptors play a critical role in some aspect of pregnancy and/or parturition. In addition, there were indications that hormonal regulation was disrupted in *Mrc1*$^{-/-}$ and *Asgr2*$^{-/-}$ mice even though they were fertile. We generated *Mrc1*$^{-/-}$*Asgr2*$^{-/-}$ mice and found that these double knock-out mice were not able to initiate parturition at the proper time, suggesting that hormonal regulation of this complex series of events was severely disrupted in these double knock-out mice. We describe here the characteristics of *Mrc1*$^{-/-}$*Asgr2*$^{-/-}$ mice as well as *Mrc1*$^{-/-}$ and *Asgr2*$^{-/-}$ mice that provide new insights into the functions of the ASGR and the ManR in reproduction as well as in other processes such as blood coagulation. The large number of plasma glycoproteins that are elevated in *Mrc1*$^{-/-}$*Asgr2*$^{-/-}$ mice indicates these receptors play important roles in many different and diverse biological functions.

Results

Mrc1$^{-/-}$*Asgr2*$^{-/-}$ *Female Mice Fail to Initiate Parturition*—*Mrc1*$^{-/-}$*Asgr2*$^{-/-}$ mice were generated by breeding male *Mrc1*$^{-/-}$*Asgr2*$^{-/-}$ mice with female *Mrc1*$^{-/-}$*Asgr2*$^{-/+}$ mice. This was necessary because 61% of pregnant *Mrc1*$^{-/-}$*Asgr2*$^{-/-}$ mice failed to initiate parturition the evening of 19.0 d.p.c. and died when parturition was initiated at a later time. When *Asgr2*$^{-/-}$ female mice were carefully monitored, we found that 35% of pregnant *Asgr2*$^{-/-}$ mice also failed to initiate parturition the evening of 19.0 d.p.c. and frequently died while attempting to deliver post-mature pups (Fig. 2*A*). In contrast, *Mrc1*$^{-/-}$ mice were not observed to have difficulty initiating or completing parturition. The number and weight of pups produced by *Asgr2*$^{-/-}$, *Mrc1*$^{-/-}$, and *Mrc1*$^{-/-}$*Asgr2*$^{-/-}$ mice were the same as WT mice following sacrifice on 18.0 and 19.0 d.p.c. Pups from *Mrc1*$^{-/-}$*Asgr2*$^{-/-}$ mice that did not initiate parturition continued to gain weight indicating they were viable and still growing. Death of the pups and the mother when parturition was initiated between 21.0 and 23.0 d.p.c. likely reflected an inability of the larger pups to transit the birth canal (Fig. 2, *panel A*). The *Asgr2*$^{-/-}$ *Mrc1*$^{-/-}$ mothers that delivered viable pups rarely succeeded in getting pregnant a second time.

The initiation of parturition is a highly coordinated and complex process that is not fully understood. Levels of the hormone relaxin increase during the later stages of pregnancy and mediate widening of the pubic symphysis to allow passage of pups through the birth canal (35). The pubic symphysis was significantly narrower in *Mrc1*$^{-/-}$*Asgr2*$^{-/-}$ than WT mice on 18.0 and 19.0 d.p.c. (Fig. 2, *panel B*). Furthermore, the symphysis of overdue *Mrc1*$^{-/-}$*Asgr2*$^{-/-}$ and *Asgr2*$^{-/-}$ mice was significantly narrower than that of 19.0 d.p.c. WT mice. Progesterone, produced by the ovary beginning on 4.0 d.p.c., is necessary for the maintenance of pregnancy following implantation. Progesterone continues to rise until 15.0 d.p.c. of pregnancy, and we have shown that this elevation drives increased expression of

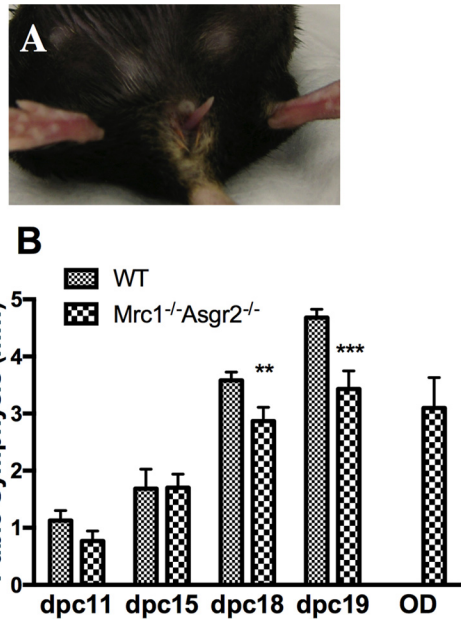

FIGURE 2. ***Mrc1*$^{-/-}$*Asgr2*$^{-/-}$ female mice were unable to initiate parturition and had narrow symphyses on P18 and P19 compared with WT mice.** *Panel A,* female *Mrc1*$^{-/-}$*Asgr2*$^{-/-}$ mice were not able to initiate parturition on 19.0 d.p.c. and were unable to deliver large post-mature pups on later dates. An example of a female *Mrc1*$^{-/-}$*Asgr2*$^{-/-}$ mouse unable to deliver her pups is shown with a tail visible in the vaginal canal. *Panel B,* timed pregnant WT and *Mrc1*$^{-/-}$*Asgr2*$^{-/-}$ mice were sacrificed on P11, P15, P18, and P19 and when 2–3 days overdue (*OD*). The pubic symphysis was exposed and its width measured. The number of mice in each group equaled 10 except for overdue mice where $n = 6$. p values for the difference in width were $p = 0.02$ on P18 and $p = 0.002$ on P19. The pubic symphyses of overdue ($n = 6$) mice were also significantly narrower than P19 ($n = 10$) mice with $p = 0.006$.

the ASGR and the ManR (9). Progesterone, ASGR, and ManR levels begin to decline late in pregnancy (9). A decrease in progesterone on 19.0 d.p.c. is essential for the initiation of parturition. RU486, an inactive analogue of progesterone, binds to the progesterone receptor and blocks the action of progesterone that is required to maintain pregnancy. RU486 induces premature parturition in WT mice when administered on 15.5 d.p.c. of pregnancy (36). We used RU486 to initiate parturition in WT, *Mrc1*$^{-/-}$, *Asgr2*$^{-/-}$, and *Mrc1*$^{-/-}$*Asgr2*$^{-/-}$ mice (10 mice per genotype). Pups were delivered within 24 h in 100% of the WT and in 100% of the *Mrc1*$^{-/-}$ mice. In contrast, parturition was induced by RU486 within 24 h in only 50% of the *Asgr2*$^{-/-}$ mice and within 48 h for the remaining 50% of the *Asgr2*$^{-/-}$ mice. RU486 induced parturition within 24 h in only 10% of the *Mrc1*$^{-/-}$*Asgr2*$^{-/-}$ mice. Of the remaining *Mrc1*$^{-/-}$*Asgr2*$^{-/-}$ mice, 40% eventually entered parturition after 48 h, whereas 50% never initiated parturition and died with post mature pups. The inability to initiate parturition at the proper time appears to be predominantly a consequence of loss of clearance by the ASGR that is further amplified by loss of clearance by the ManR and cannot be overcome by administration of RU486.

Male *Mrc1*$^{-/-}$*Asgr2*$^{-/-}$ mice also manifested abnormalities that were not seen in either *Asgr2*$^{-/-}$ or *Mrc1*$^{-/-}$ mice. Twenty five percent of male *Mrc1*$^{-/-}$*Asgr2*$^{-/-}$ mice placed with female mice for the purpose of breeding developed priapism (Fig. 3, *panel A*) and had to be sacrificed to prevent infection. Cross-sections of the phallus revealed that the penile vein in male mice with priapism was thrombosed (compare WT in Fig. 3, *panel B,*

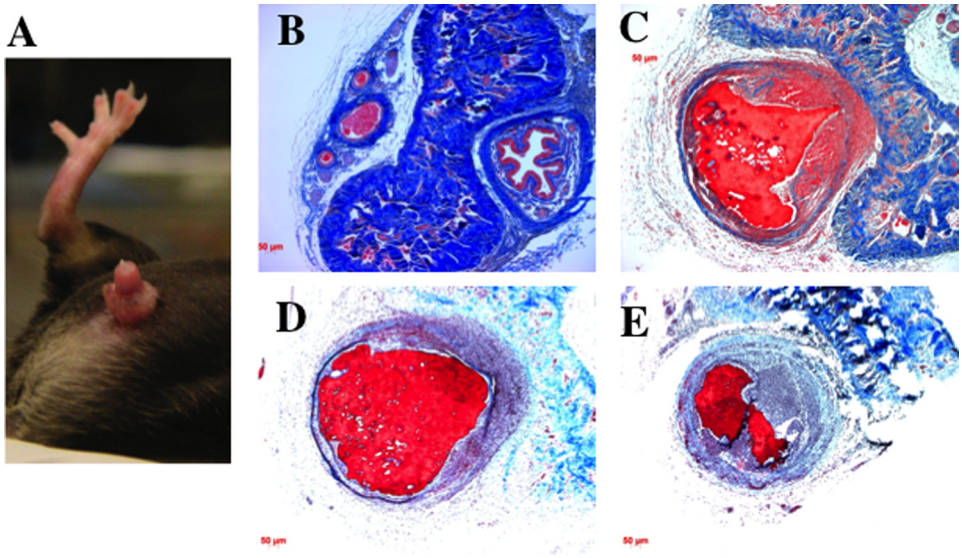

FIGURE 3. **Male *Mrc1*$^{-/-}$*Asgr2*$^{-/-}$ mice developed priapism due to thrombosis of the penile vein.** *Panel A,* 25% of *Mrc1*$^{-/-}$*Asgr2*$^{-/-}$ male mice developed priapism when placed with female mice for breeding. An example of a male *Mrc1*$^{-/-}$*Asgr2*$^{-/-}$ mouse with priapism is shown. Sections from WT (*panel B*) and *Mrc1*$^{-/-}$*Asgr2*$^{-/-}$ mice (*panels C–E*) revealed that the penile vein was thrombosed. *Panels C–E,* present progressively older thrombi as indicated by the presence of increasing numbers of polymorphonuclear leukocytes. Increased numbers of red blood cells can be seen in the corpora cavernosa of *Mrc1*$^{-/-}$ *Asgr2*$^{-/-}$ mice compared with WT mice (compare *panels B* and *C*).

with *Mrc1*$^{-/-}$*Asgr2*$^{-/-}$ in *panels C–E*). The thrombi varied in age with some being acute (Fig. 3, *panel C*), and others demonstrated a major influx of neutrophils (Fig. 3, *panels D* and *E*) indicating the thrombus had developed 24–48 h before sacrifice. Priapism was never observed in either *Asgr2*$^{-/-}$ or *Mrc1*$^{-/-}$ mice. Thus, lack of clearance by both the ASGR and the ManR in male mice has an impact that is not seen in the absence of clearance by only one of the two receptors.

Clearance of Endogenous LH in Asgr2$^{-/-}$*, Mrc1*$^{-/-}$*, and Mrc1*$^{-/-}$*Asgr2*$^{-/-}$ *Mice*—The glycoprotein hormone LH bears *N*-linked glycans that terminate with β1,4-linked GalNAc-4-SO_4 (37–40), whereas FSH bears *N*-linked glycans that terminate with Siaα2,3/6Gal (see Fig. 1) (37–39). The ManR expressed by SEC mediates the clearance of glycoproteins bearing two or more *N*-glycans with terminal GalNAc-4-SO_4 (1, 9, 22, 23, 41). Following ablation of GalNAc-4-sulfotransferase-1 (*CHST8, GalNAc-4-ST1*), *GalNAc-4-ST1*$^{-/-}$ mice produce LH that terminates with Siaα2,6GalNAc instead of GalNAc-4-SO_4, resulting in a longer half-life *in vivo* and increased circulating levels (32). We therefore expected that the half-life of endogenous LH would also be prolonged in *Mrc1*$^{-/-}$ mice as compared with WT mice and that *Mrc1*$^{-/-}$ mice would manifest changes in their regulation of estrogen and testosterone production.

We recently compared the clearance of an exogenous recombinant glycoprotein bearing multiple *N*-linked glycans in WT, *Asgr2*$^{-/-}$, *Mrc1*$^{-/-}$, and *Mrc1*$^{-/-}$*Asgr2*$^{-/-}$ mice, and we demonstrated that the ManR accounts for clearance of exogenous glycoproteins bearing terminal GalNAc-4-SO_4 on *N*-linked glycans (1, 9, 23). Our present studies compared the clearance rates for endogenous LH that bears glycans terminating with GalNAc-4-SO_4 in WT, *Asgr2*$^{-/-}$, *Mrc1*$^{-/-}$, and *Mrc1*$^{-/-}$ *Asgr2*$^{-/-}$ mice by acutely blocking secretion of LH in castrated male mice with acyline and following the decrease in circulating LH with time as described previously (32). Endogenous LH was cleared with a half-life of 8 and 7.5 min, respectively, in WT and *Asgr2*$^{-/-}$ mice (Fig. 4, *panels A, B,* and *E*). In contrast, LH was cleared with a half-life of 15 and 12 min, respectively, in *Mrc1*$^{-/-}$ and *Mrc1*$^{-/-}$*Asgr2*$^{-/-}$ mice (Fig. 4, *panels C–E*). This prolongation of half-life demonstrates that the ManR does indeed account for the rapid clearance of endogenous LH *in vivo*.

Measurement of circulating LH, FSH, and testosterone levels in WT, *Mrc1*$^{-/-}$, *Asgr2*$^{-/-}$, and *Mrc1*$^{-/-}$*Asgr2*$^{-/-}$ male mice revealed LH levels that were significantly elevated in *Mrc1*$^{-/-}$, *Asgr2*$^{-/-}$, and *Mrc1*$^{-/-}$*Asgr2*$^{-/-}$ mice compared with WT mice (Fig. 5, *panels A–C*) and demonstrated greater variability (Fig. 5, *panel A*). In contrast, circulating FSH levels did not differ significantly in *Mrc1*$^{-/-}$, *Asgr2*$^{-/-}$, and *Mrc1*$^{-/-}$ *Asgr2*$^{-/-}$ mice compared with WT mice, although *Asgr2*$^{-/-}$ mice did demonstrate greater variability compared with WT mice (Fig. 5, *panel B*). In agreement with the elevated levels of LH, testosterone levels were also elevated in *Mrc1*$^{-/-}$, *Asgr2*$^{-/-}$, and *Mrc1*$^{-/-}$*Asgr2*$^{-/-}$ mice. Furthermore, the size of seminal vesicles, which is sensitive to testosterone levels, was significantly greater in *Mrc1*$^{-/-}$, *Asgr2*$^{-/-}$, and *Mrc1*$^{-/-}$ *Asgr2*$^{-/-}$ mice than in WT mice, consistent with the elevated testosterone levels (Fig. 5, *panels C* and *D*).

Thus ablation of the ManR (*Mrc1*) resulted in increased levels of circulating LH by prolonging the half-life for LH (Figs. 4, *panel C,* and 5, *panel A*). Unexpectedly, loss of clearance by the ASGR following ablation of *Asgr2* also resulted in increased levels of circulating LH and testosterone (Fig. 5, *panels A* and *B*), even though the half-life for LH clearance was not altered from that of WT (see Fig. 4, *panels B* and *E*). These phenotypic changes seen in the *Asgr2*$^{-/-}$ and *Mrc1*$^{-/-}$*Asgr2*$^{-/-}$ male mice suggest that an unidentified glycoprotein that would normally be cleared by the ASGR acts as a positive regulator of LH production and release by the pituitary.

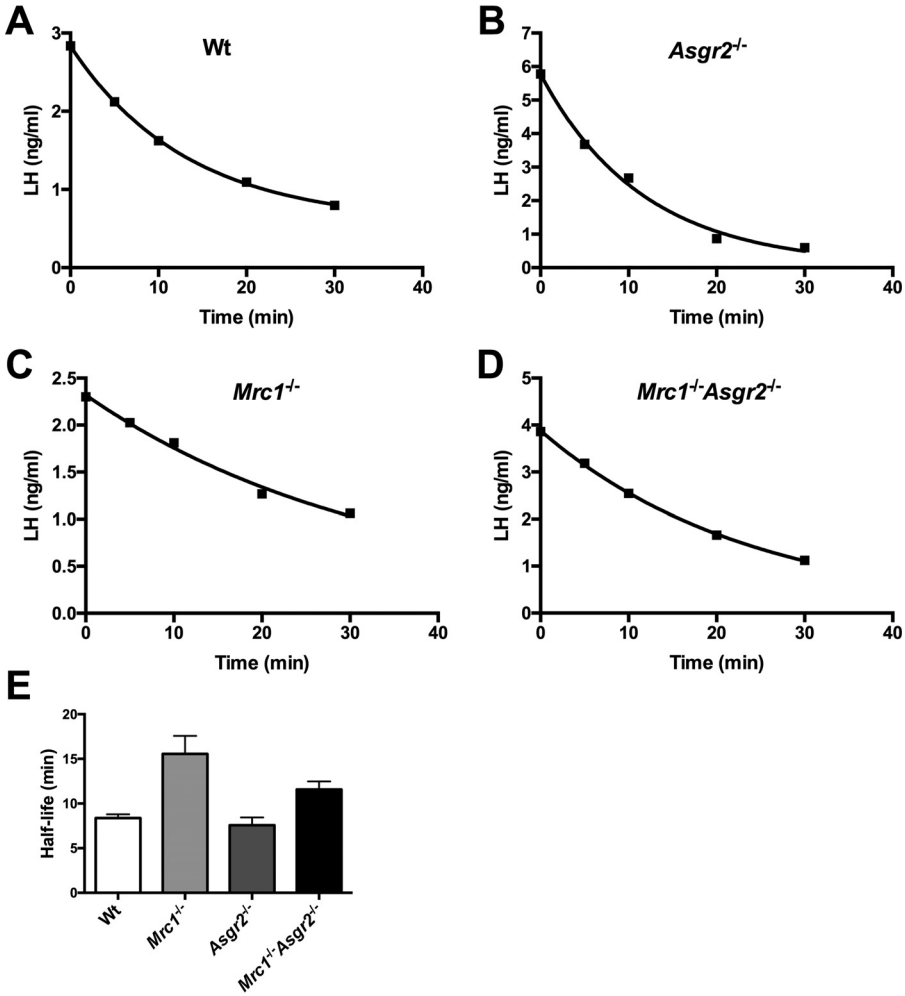

FIGURE 4. **Clearance of LH is prolonged in *Mrc1*$^{-/-}$ and *Mrc1*$^{-/-}$*Asgr2*$^{-/-}$ mice.** WT ($n = 5$), *Mrc1*$^{-/-}$ ($n = 9$), *Asgr2*$^{-/-}$ ($n = 9$), and *Mrc1*$^{-/-}$*Asgr2*$^{-/-}$ ($n = 12$) male mice were castrated. Five days later, mice were injected retro-orbitally with 10 μg of acyline, and blood was collected at 0, 5,10, 20, and 30 min. The amount of LH (ng/ml) in the plasma at each time point was determined by radioimmunoassay. Examples of clearance curves are shown for WT (*panel A*), *Mrc1*$^{-/-}$ (*panel B*), *Asgr2*$^{-/-}$ (*panel C*), and *Mrc1*$^{-/-}$*Asgr2*$^{-/-}$ (*panel D*). Half-lives were determined by non-linear regression using Prism 6.0. The mean and S.E. for the half-lives determined for each group are shown in *panel E*. The half-life was significantly prolonged compared with WT in both *Mrc1*$^{-/-}$ (8.4 min *versus* 15.6 min, $p = 0.02$) and *Mrc1*$^{-/-}$*Asgr2*$^{-/-}$ mice (8.4 *versus* 11.6 min, $p = 0.04$) but was not significantly changed in *Asgr2*$^{-/-}$ mice. *p* values were determined by unpaired *t* test.

We examined the pituitaries of male *Mrc1*$^{-/-}$, *Asgr2*$^{-/-}$, and *Mrc1*$^{-/-}$*Asgr2*$^{-/-}$ mice to determine whether loss of clearance by the ManR and/or the ASGR has an impact on glycoprotein hormone production and/or modification. The increase in LHβ mRNA levels we observed in *Mrc1*$^{-/-}$ mice (Fig. 6, *panel A*) was unexpected because increased plasma testosterone levels (Fig. 5, *panel C*) in response to lengthened LH half-life was more likely to exert the known feedback effect of decreasing LH production/release in the pituitary. LHβ mRNA levels increased even more in *Asgr2*$^{-/-}$ mice (Fig. 6, *panel A*) even though their plasma testosterone was elevated (Fig. 5, *panel C*). The LHβ mRNA elevation in *Asgr2*$^{-/-}$ mice provides further support for a positive regulator of LH production that is normally cleared by the ASGR. Plasma LH and testosterone levels were elevated in *Mrc1*$^{-/-}$*Asgr2*$^{-/-}$ mice to a similar level as in the single knock-out mice (Fig. 5, *panels A* and *C*), yet LHβ mRNA levels were 3.0-fold lower in *Mrc1*$^{-/-}$*Asgr2*$^{-/-}$ mice than *Asgr2*$^{-/-}$ mice (Fig. 6, *panel A*). Whereas for TSH, which like LH, bears glycans terminating in GalNAc-4-SO_4 (37, 38), little change in TSHβ mRNA levels was observed in single knock-out mice, whereas a 2–3-fold decrease was again seen in *Mrc1*$^{-/-}$*Asgr2*$^{-/-}$ mice compared with either WT or *Asgr2*$^{-/-}$ mice (Fig. 6, *panel B*). FSH does not bear structures that are recognized by either the ManR or the ASGR (see Fig. 1) (37, 38). FSHβ mRNA levels did not change in either *Mrc1*$^{-/-}$ or *Asgr2*$^{-/-}$ mice but did decrease nominally in *Mrc1*$^{-/-}$*Asgr2*$^{-/-}$ mice (Fig. 6, *panel C*). The profile of decreases in pituitary glycoprotein hormone mRNA synthesis in *Mrc1*$^{-/-}$*Asgr2*$^{-/-}$ mice points to a broader impact of the concurrent absence of both clearance receptors.

We also observed changes in pituitary transcript levels for the glycosyltransferases that are responsible for the addition of GalNAc in β1,4-linkage to *N*-linked glycans (B4galnt3 and B4galnt4) and modification of the β1,4-linked GalNAc with either SO_4 (Galnac4st1) or sialic acid (St6gal1) (see Fig. 1). Loss of clearance by either the ManR or the ASGR resulted in a 1.5–2.0-fold increase in Galnac4st1 and St6gal1 transcript levels (Fig. 7, *panels A* and *B*). In contrast, loss of clearance by both the ManR and the ASGR in double knock-out mice reduced transcript levels not only for LHβ and TSHβ (Fig. 6,

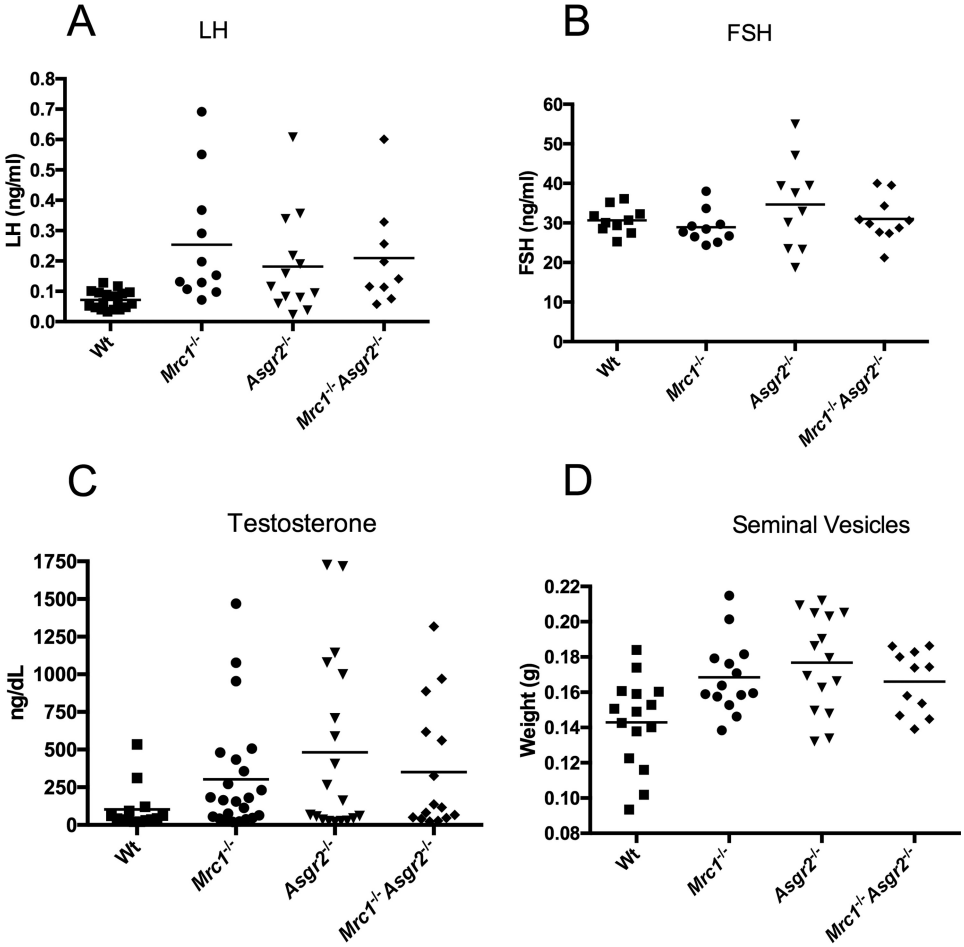

FIGURE 5. **LH and testosterone but not FSH are elevated in *Mrc1*$^{-/-}$, *Asgr2*$^{-/-}$, and *Mrc1*$^{-/-}$*Asgr2*$^{-/-}$ mice.** Plasma was collected from adult male WT, *Mrc1*$^{-/-}$, *Asgr2*$^{-/-}$, and *Mrc1*$^{-/-}$*Asgr2*$^{-/-}$ mice. Circulating LH levels (*panel A*) were determined using an immunoradiometric assay and analyzed using a parametric *t* test. LH levels were significantly elevated in all three genotypes compared with WT ($p < 0.005$). Testosterone levels (*panel B*) were determined by RIA and analyzed using a non-parametric *t* test, Mann-Whitney, because testosterone does not follow a normal distribution. Testosterone was significantly elevated in all three genotypes compared with WT ($p < 0.05$). FSH levels (*panel C*) were determined by RIA. There was no significant difference between WT and any of the genotypes. Seminal vesicles (*panel D*) were dissected and weighed. Seminal vesicle size was determined by testosterone level and was significantly increased in all three genotypes: $p = 0.006$ for *Mrc1*$^{-/-}$, $p = 0.002$ for *Asgr2*$^{-/-}$, and $p = 0.02$ for *Mrc1*$^{-/-}$*Asgr2*$^{-/-}$ mice.

panels A and *B*) but also 1.8–2.2-fold for Galnac4st1 and 4.6–5.8-fold for St6gal1 as compared with either of the single knock-out mice (Fig. 7, *panels A* and *B*). Loss of clearance by the ManR, the ASGR, or both receptors in double knock-out mice resulted in a small but significant decrease in B4galnt3 or B4galnt4 transcript levels (Fig. 7, *panels C* and *D*). The pituitary contains multiple different cell types, so the changes seen in transcript levels may be far greater for these transferases in the specific cell types that synthesize LH, TSH, and FSH. Changes in the relative levels of LH and TSH, as well as their modifying enzymes GalNAc-4-ST1 and ST6Gal1, could alter the pattern of LH and TSH glycan terminal modification with SO_4 and sialic acid and thus have an impact on clearance rates *in vivo*.

We examined the testis, a target tissue for LH action, for changes in transcript levels of genes that would be relevant to testosterone production, because Leydig cells in the testes respond to increased LH levels by increasing testosterone production. Steady state transcript levels for the LH receptor, steroidogenic acute regulatory protein (StAR), 20α-hydroxysteroid dehydrogenase (20αHSD), activin, and inhibin were determined in WT, *Mrc1*$^{-/-}$, *Asgr2*$^{-/-}$, and *Mrc1*$^{-/-}$ *Asgr2*$^{-/-}$ mice to see whether there were any changes consistent with LH-driven increases in testosterone production (Fig. 8). There was little change in transcript levels for any of these genes in either *Mrc1*$^{-/-}$ or *Asgr2*$^{-/-}$ mice compared with WT mice; however, there was a striking increase in the transcript levels for each of these genes in *Mrc1*$^{-/-}$*Asgr2*$^{-/-}$ mice. Particularly notable were the increased levels of mRNA for 20α-hydroxysteroid dehydrogenase (14-fold), activin (4-fold), and inhibin (6-fold). In *Mrc1*$^{-/-}$*Asgr2*$^{-/-}$ mice, these substantial increases in testicular components of the testosterone synthetic pathway and regulatory proteins, coupled with elevated circulating testosterone levels and a major decrease in LHβ mRNA (Fig. 6, *panel A*), underscore the more widespread disruption of reproductive hormone homeostasis that occurs when both major glycan-mediated recognition and clearance pathways are ablated.

Circulating Glycoproteins Elevated in Pregnant Asgr2$^{-/-}$ *Mrc1*$^{-/-}$ *Mice*—Because *Asgr2*$^{-/-}$*Mrc1*$^{-/-}$ mice were not able to initiate parturition, we utilized mass spectrometry to analyze the plasma from *Asgr2*$^{-/-}$*Mrc1*$^{-/-}$ and WT mice on 18.5 d.p.c.

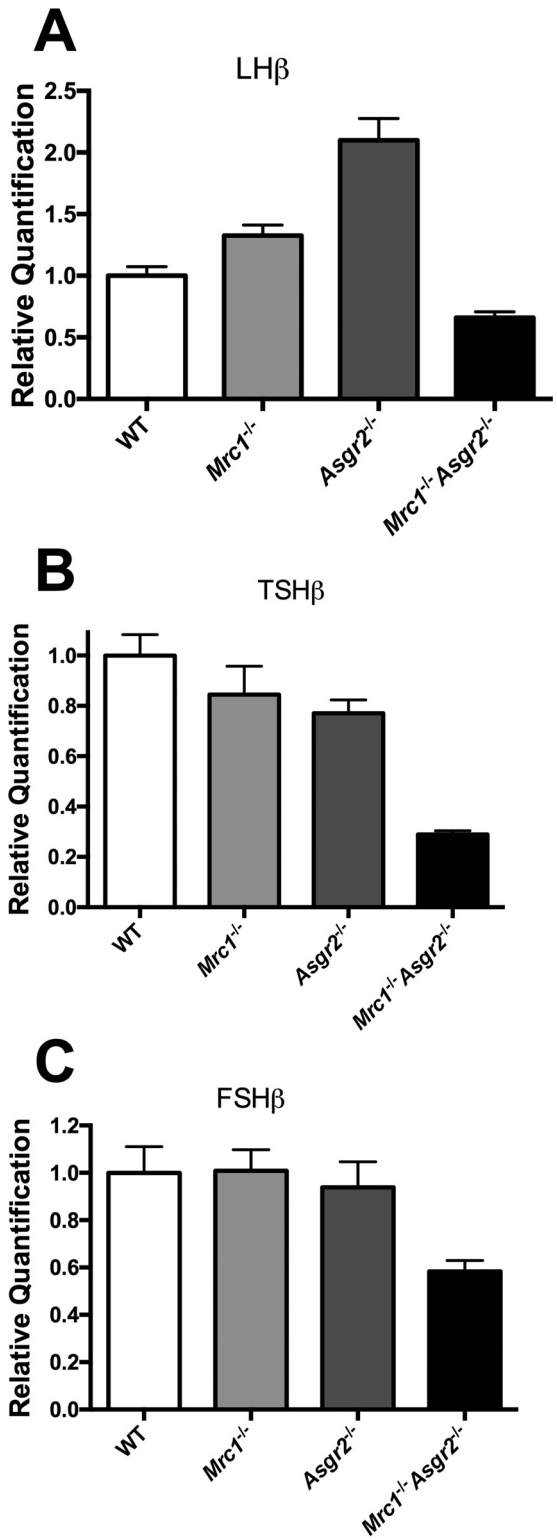

FIGURE 6. **LHβ, TSHβ, and FSHβ mRNA levels are altered in the pituitaries of *Mrc1*$^{-/-}$, *Asgr2*$^{-/-}$, and *Mrc1*$^{-/-}$*Asgr2*$^{-/-}$ mice.** Pituitaries were collected from adult male WT ($n = 7$), *Mrc1*$^{-/-}$ ($n = 7$), *Asgr2*$^{-/-}$ ($n = 7$), and *Mrc1*$^{-/-}$*Asgr2*$^{-/-}$ ($n = 5$) mice, and the relative quantity of mRNA was determined by PCR. mRNA levels differed significantly from those of WT mice as follows: *panel A*, LHβ in *Mrc1*$^{-/-}$ ($p = 0.02$); *Asgr2*$^{-/-}$ ($p = 0.0001$); and *Mrc1*$^{-/-}$*Asgr2*$^{-/-}$ ($p = 0.006$) mice. *Panel B*, TSHβ in *Asgr2*$^{-/-}$ ($p = 0.04$) and *Mrc1*$^{-/-}$*Asgr2*$^{-/-}$ ($p = 0.0001$) mice, and *panel C*, FSHβ in *Mrc1*$^{-/-}$*Asgr2*$^{-/-}$ ($p = 0.01$) mice.

of pregnancy for altered levels of circulating proteins that might be contributing to this condition. At least 90 plasma proteins were elevated 2.0-fold or more in *Asgr2*$^{-/-}$*Mrc1*$^{-/-}$ as compared with WT mice (supplemental Table I). Among the proteins for which ≥5 spectra were obtained from *Asgr2*$^{-/-}$*Mrc1*$^{-/-}$ mice, there were 28 instances where no spectra were obtained from the WT mice indicating concentrations below the level of detection by mass spectrometry. Forty proteins were elevated >3.0-fold and an additional 22 were elevated between 2.0- and 3.0-fold in *Asgr2*$^{-/-}$*Mrc1*$^{-/-}$ compared with WT mice. Proteins that were elevated included pregnancy-specific glycoproteins (PSGs), coagulation factors, lysosomal proteins, and collagens. A large number of plasma proteins were not significantly elevated in *Asgr2*$^{-/-}$*Mrc1*$^{-/-}$ as compared with WT mice. Among them were acute phase proteins such as C-reactive protein and ceruloplasmin, indicating that pregnant *Asgr2*$^{-/-}$*Mrc1*$^{-/-}$ mice did not show evidence of a generalized increase in inflammatory response as compared with WT mice. The large number of different glycoproteins that are elevated in *Asgr2*$^{-/-}$*Mrc1*$^{-/-}$ mice indicates that the ASGR and the ManR contribute to the regulation of a wide range of glycoproteins. It is likely that the clearance of many additional proteins is also controlled by the ASGR and the ManR, but even when elevated in *Asgr2*$^{-/-}$*Mrc1*$^{-/-}$ mice, their levels fall below that required for detection by mass spectrometry.

Mass spectrometry indicated that multiple PSGs were elevated in the plasma of *Asgr2*$^{-/-}$*Mrc1*$^{-/-}$ as compared with WT mice (Table 1). To confirm that circulating PSG23 was elevated in *Asgr2*$^{-/-}$*Mrc1*$^{-/-}$ mice and to determine which receptor accounted for the clearance of PSG23, we performed Western blot analyses using plasma from WT, *Asgr2*$^{-/-}$, *Mrc1*$^{-/-}$, and *Asgr2*$^{-/-}$*Mrc1*$^{-/-}$ mice. PSG23 was detected in the plasma of *Asgr2*$^{-/-}$*Mrc1*$^{-/-}$ and *Asgr2*$^{-/-}$ mice but not in the plasma from either WT or *Mrc1*$^{-/-}$ mice (Fig. 9, *panels A* and *C*). Prolonged exposure of the Western blot did not reveal any PSG23 in the plasma of WT and *Mrc1*$^{-/-}$ mice (Fig. 9, *panel C*). In contrast, extracts of placenta from WT, *Asgr2*$^{-/-}$, *Mrc1*$^{-/-}$, and *Asgr2*$^{-/-}$*Mrc1*$^{-/-}$ mice contained similar amounts of PSG23 (Fig. 9, *panel B*). Thus, the absence of PSG23 in plasma of WT and *Mrc1*$^{-/-}$ mice reflects rapid clearance by the ASGR rather than a change in PSG23 protein production in its placental source.

To obtain an indication of the capacity and efficiency of the ASGR for clearing glycoproteins bearing its recognized glycans, we determined how much PSG23 was present in the plasma from WT and *Asgr2*$^{-/-}$*Mrc1*$^{-/-}$ mice. Quantitative Western blot analyses comparing dilutions of known quantities of recombinant PSG23 with PSG23 in the plasma of *Asgr2*$^{-/-}$*Mrc1*$^{-/-}$ mice revealed that the amount of PSG23 in WT plasma was less than 50 ng/ml, whereas the amount of PSG23 in *Asgr2*$^{-/-}$*Mrc1*$^{-/-}$ plasma was in the range of 1–10 mg/ml plasma. The ASGR is therefore able to reduce the concentration of PSG23 from 10 mg/ml found in the absence of clearance in *Asgr2*$^{-/-}$*Mrc1*$^{-/-}$ double knock-out or *Asgr2*$^{-/-}$ single knock-out to less than 50 ng/ml in WT mice.

PSG23 is extensively glycosylated with seven *N*-glycans that are distributed over three Ig motifs (42). The elevated levels of circulating PSG23 and other PSGs seen in *Asgr2*$^{-/-}$ and

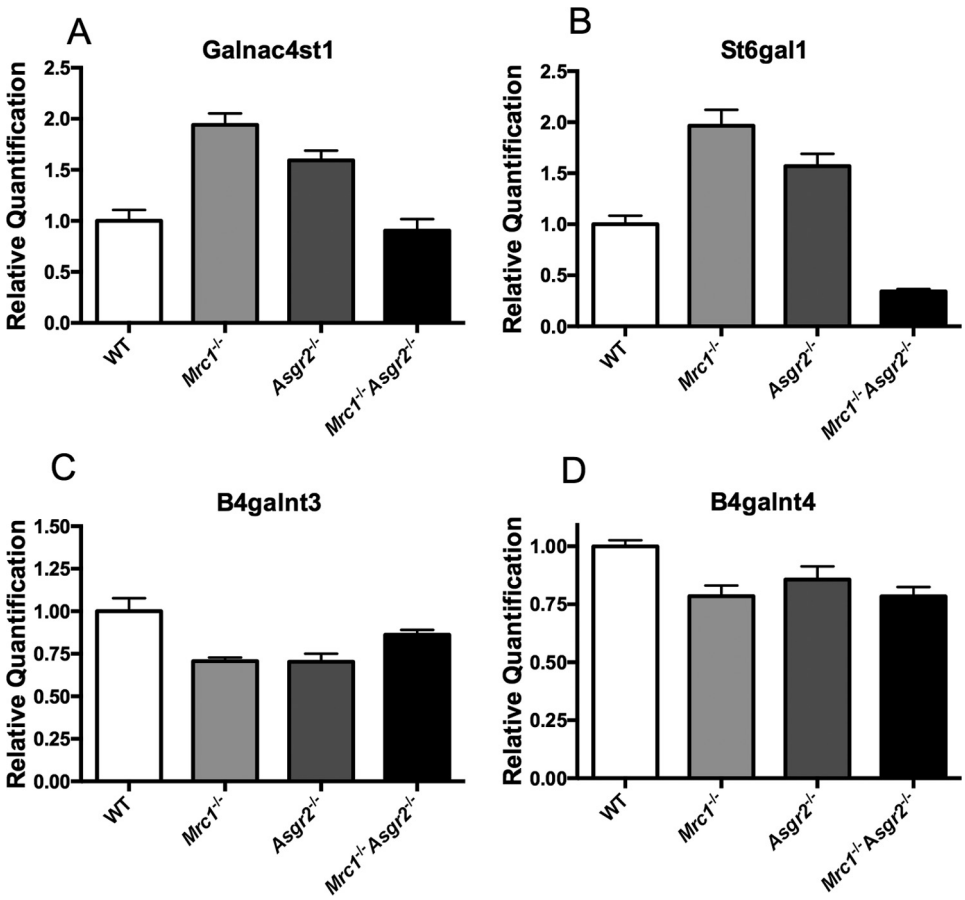

FIGURE 7. **Galnac4st1, St6gal, B4galnt3, and B4galnt4 mRNA levels are altered in the pituitaries of *Mrc1*$^{-/-}$, *Asgr2*$^{-/-}$, and *Mrc1*$^{-/-}$*Asgr2*$^{-/-}$ mice.** Pituitaries were collected from adult male WT ($n = 7$), *Mrc1*$^{-/-}$ ($n = 7$), *Asgr2*$^{-/-}$ ($n = 7$), and *Mrc1*$^{-/-}$*Asgr2*$^{-/-}$ ($n = 5$) mice, and the relative quantity of mRNA was determined by PCR. mRNA levels differed significantly from those of WT mice as follows. *Panel A,* galnac4st1 in *Mrc1*$^{-/-}$ ($p = 0.0001$) and *Asgr2*$^{-/-}$ ($p = 0.001$) mice. *Panel B,* St6gal1 in *Mrc1*$^{-/-}$ ($p = 0.0002$), *Asgr2*$^{-/-}$ ($p = 0.002$), and *Mrc1*$^{-/-}$*Asgr2*$^{-/-}$ ($p = 0.0001$) mice. *Panel C,* B4galnt3 for *Mrc1*$^{-/-}$ ($p = 0.01$) and *Asgr2*$^{-/-}$ ($p = 0.02$) but not *Mrc1*$^{-/-}$*Asgr2*$^{-/-}$ mice. *Panel D,* B4galnt4 for *Mrc1*$^{-/-}$ ($p = 0.007$) and *Mrc1*$^{-/-}$*Asgr2*$^{-/-}$ ($p = 0.004$) but not *Asgr2*$^{-/-}$ mice.

Asgr2$^{-/-}$*Mrc1*$^{-/-}$ mice but not in WT or *Mrc1*$^{-/-}$ mice indicated that PSGs bear glycans that are recognized by the ASGR, for example, *N*-linked glycans terminating with either Galβ1,4GlcNAc or GalNAcβ1,4GlcNAc as well as glycans terminating with Galβ1,4[Fucα1,3]GlcNAc known as Lewis^x or GalNAcβ1,4[Fucα1,3]GlcNAc (see Fig. 1) (9, 43). During glycan synthesis, terminal β1,4-linked Gal or GalNAc is typically further modified with sialic acid or in the case of GalNAc with SO_4; however, the presence of Fuc on the underlying GlcNAc prevents the addition of sialic acid. In a recent study, we utilized recombinant PSG23 bearing each of the *N*-glycans shown in Fig. 1 to demonstrate that the ASGR mediated clearance of PSG23 bearing glycans terminating with either β1,4-linked Gal or GalNAc in the presence or absence of an underlying Fuc, and that the addition of either sialic acid or sulfate prevented clearance by the ASGR (9).

Immobilized plant lectins can be utilized to differentiate among many of the *N*-glycan structures shown in Fig. 1 (44, 45) as summarized in Fig. 10. To gain insight into the structure of the *N*-glycans on endogenous PSG23, we compared the behavior of PSG23 present in the plasma of *Asgr2*$^{-/-}$*Mrc1*$^{-/-}$ mice with that of recombinant PSG23 bearing glycans of known structure during digestion with glycosidases of known specificity and during lectin affinity chromatography. *Wisteria floribunda* agglutinin (WFA) binds glycans with terminal β1,4-linked GalNAc but not those with β1,4-linked Gal, whereas *Ricinus communis* agglutinin-I (RCA_I) binds glycans with terminal β1,4-linked Gal but not those with β1,4-linked GalNAc (45–48). PSG23 from *Asgr2*$^{-/-}$*Mrc1*$^{-/-}$ mice was bound by RCA_I-agarose but not by WFA-agarose (Fig 10, *panel C*), indicating that terminal β1,4-linked Gal but not GalNAc was present on its *N*-glycans. It should be noted that glycoproteins such as PSG23 modified with multiple *N*-glycans are not readily eluted from the immobilized lectin using competitive mono- or disaccharides. The bound PSG23 can, however, be eluted by boiling in loading buffer for SDS-PAGE. The binding can be demonstrated to be lectin-dependent by incubation with the immobilized lectin in the absence or presence of lactose that prevents binding (see Fig. 10, *panel E,* for example).

Binding of PSG23 by immobilized RCA_I but not WFA indicated that terminal β1,4-linked Gal rather than GalNAc was present on the PSG23 *N*-glycans. Digestion with neuraminidase resulted in a small shift in the mobility of PSG23 that can be best appreciated in Fig. 10, *panel B*, indicating a small amount of terminal sialic acid was present. However, following digestion with neuraminidase, binding to immobilized WFA and RCA_I was unchanged (Fig. 10, *panel D*) indicating that neither β1,4-linked GalNAc nor Siaα2,6GalNAc was present.

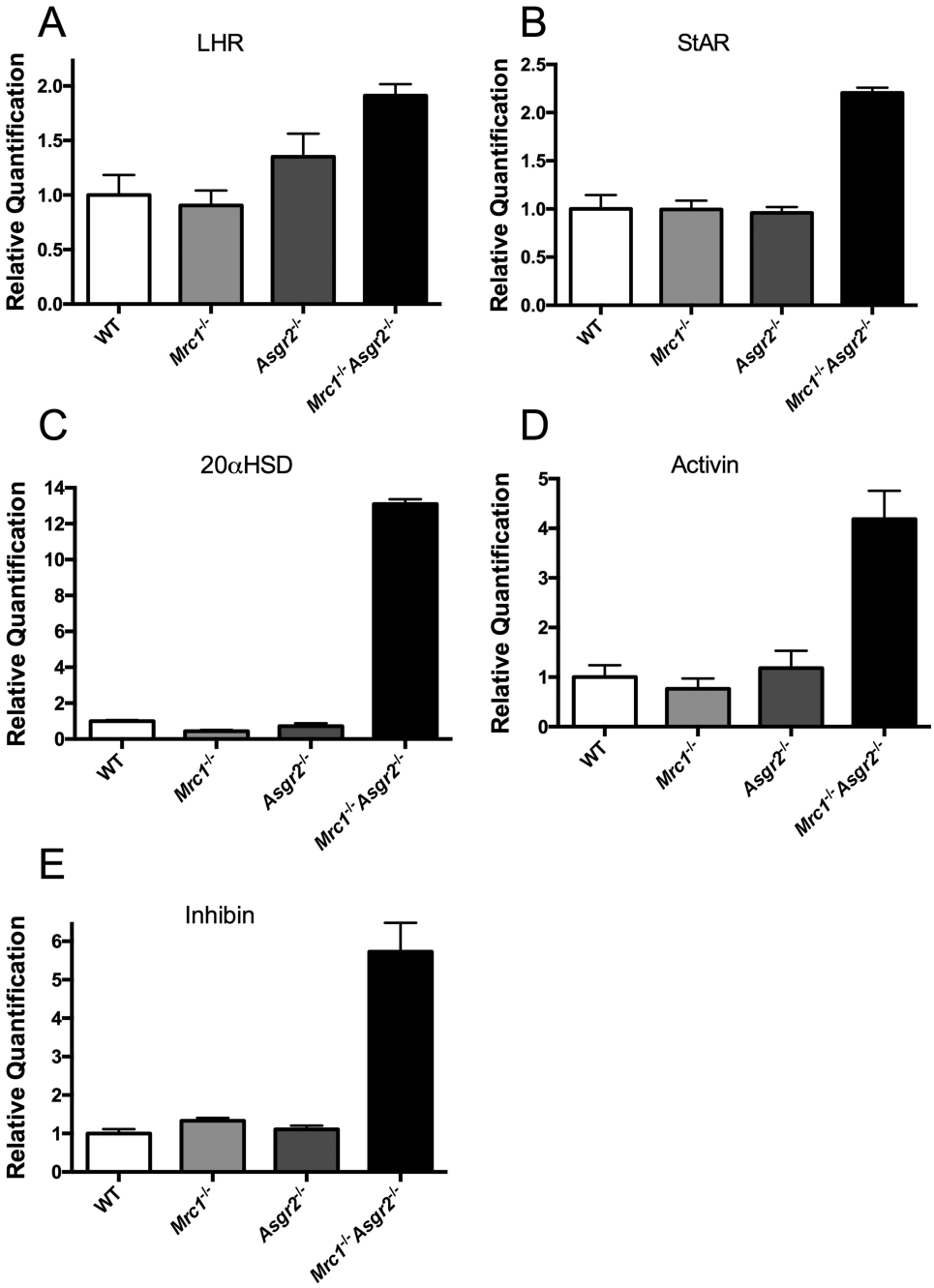

FIGURE 8. **Alterations in LH receptor, steroidogenic acute regulatory protein, 20α-hydroxysteroid dehydrogenase, activin, and inhibin mRNA levels in the testes of *Mrc1*$^{-/-}$, *Asgr2*$^{-/-}$, and *Mrc1*$^{-/-}$*Asgr2*$^{-/-}$ mice.** Testes were collected from adult male WT ($n = 4$), *Mrc1*$^{-/-}$ ($n = 4$), *Asgr2*$^{-/-}$ ($n = 4$), and *Mrc1*$^{-/-}$*Asgr2*$^{-/-}$ ($n = 4$) mice, and the relative quantity of mRNA was determined by PCR. mRNA levels differed from those of WT mice as follows. *Panel A,* LH receptor (*LHR*) in *Mrc1*$^{-/-}$*Asgr2*$^{-/-}$ ($p = 0.005$) mice but not in *Mrc1*$^{-/-}$ or *Asgr2*$^{-/-}$ mice. *Panel B,* StAR in *Mrc1*$^{-/-}$*Asgr2*$^{-/-}$ ($p = 0.0002$) mice but not in *Mrc1*$^{-/-}$ or *Asgr2*$^{-/-}$ mice. *Panel C,* 20αHSD in *Mrc1*$^{-/-}$ ($p = 0.001$) and *Mrc1*$^{-/-}$*Asgr2*$^{-/-}$ ($p = 0.0001$) mice but not *Asgr2*$^{-/-}$ mice. *Panel D,* activin in *Mrc1*$^{-/-}$*Asgr2*$^{-/-}$ ($p = 0.002$) mice but not in either *Mrc1*$^{-/-}$ or *Asgr2*$^{-/-}$ mice. *Panel E,* inhibin in *Mrc1*$^{-/-}$ ($p = 0.05$) and *Mrc1*$^{-/-}$*Asgr2*$^{-/-}$ ($p = 0.0008$) mice but not *Asgr2*$^{-/-}$ mice.

Clearance by the ASGR and binding by immobilized RCA_I indicated the presence of β1,4-linked Gal. However, digestion with β-galactosidase did not alter the migration of endogenous PSG23 on SDS-PAGE (Fig. 10, *panels A* and *B*) or binding by immobilized RCA_I (Fig. 10, *panels A, B,* and *E*). The β-galactosidase produced by *Diplococcus pneumoniae* is highly specific. This enzyme releases the β1,4-linked Gal from Galβ1,4GlcNAc but not from the Lewis^X structure Galβ1,4[Fucα1,3]GlcNAc, as we previously confirmed with recombinant PSG23. In those studies, binding of recombinant PSG23 bearing Galβ1, 4GlcNAc to RCA_I-agarose was abolished by digestion with diplococcal β-galactosidase, whereas binding of recombinant PSG23 bearing Lewis^X structure Galβ1,4[Fucα1,3]GlcNAc was not affected by digestion with diplococcal β-galactosidase (9). Thus, it is likely that the endogenous PSG23 analyzed here bears the Lewis^X structure. Multiple monoclonal antibodies specific for the Lewis^X structure from commercial sources and generously provided by colleagues (49) were tested as potential

TABLE 1
Selected groups of plasma proteins elevated on 18.5 d.p.c. of pregnancy in *Mrc1*$^{-/-}$*Asgr2*$^{-/-}$ mice
INF, infinite.

Protein	Accession no.	Molecular mass	-Fold change	WT	KO
		kDa			
CEA-related					
PSG27	Q497W2	54	51	2	101
PSG30 (CEACAM5)	Q3UKK2	106	90	1	87
PSG23	Q9D2UO	53	22	3	66
PSG21	Q9DAV5	53	21	2	42
CEACAM12	Q3UKP4	34	13	2	25
CEACAM11	Q9D0Z8	34	INF	0	17
PSG16	Q8KOU8	45	27	1	14
CEACAM14	Q78Y72	29	INF	0	6
PSG28	Q4KL66	53	INF	0	2
PSG18	B2RSG7	54	INF	0	1
Coagulation					
Von Willebrand factor	Q8CIZ8	309	7.0	1	7
Coagulation Factor XIIIA	Q8BH61	83	6.8	4	27
Coagulation Factor V	O88783	247	2.2	81	178
Transforming growth factor-β-induced protein ig-h3	P82198	75	12	1	12
Platelet glycoprotein V (fragment)	Q9QZU3	63	INF	0	6
Platelet glycoprotein 1b α chain	O35930	80	3.7	6	22
Platelet-activating factor acetylhydrolase	Q60963	49	3.1	12	37
Thrombospondin-4	Q9Z1T2	106	INF	0	30
Collagens					
Collagen α-1(VI) chain	Q04857	108	INF	0	33
Collagen α-2(V) chain	Q3U962	145	INF	0	19
Collagen α-1(V) chain	O88207	184	INF	0	15
Collagen α-1(XI) chain	Q61245	181	INF	0	14
Collagen α-2(XI) chain	Q64739	172	INF	0	6
Collagen α-1(I) chain	P11087	138	3.5	10	35
Collagen α-2(I) chain	Q01149	130	3.4	7	24
Collagen α-1(III) chain	P08121	139	2.2	5	11
Lysosomal proteins					
N-Acetylgalactosamine-6-sulfatase	Q571E4	58	INF	0	15
γ-Interferon-induced lysosomal thiol reductase	Q9ESY9	28	INF	0	6
β-Hexosaminidase subunit β	P20060	61	INF	0	4
Lysosomal Pro-X carboxypeptidase	Q7TMR0	55	INF	0	4
Lysosomal acid lipase/cholesterol ester hyrolase	Q9Z0M5	45	INF	0	3
Cathepsin D	P18242	45	4.0	3	12
Lysosomal α-mannosidase	O09159	115	1.7	14	24
Miscellaneous					
Serum amyloid P-component	P12246	26	3.3	39	129
C-reactive protein	P14847	25	1.0	39	39

probes for the Lewis^X structure on *N*-linked glycans using our recombinant PSG23 known to bear this structure. Whereas some monoclonals (49) were active against the Lewis^X structure on *O*-linked glycans, none were active against the Lewis^X structure on *N*-linked glycans; thus, these reagents were not usable for analyzing the Lewis^X structure on endogenous PSG23. Digestion of plasma with endoglycosidase H did not change the mobility of PSG23 (Fig. 10, *panel A*) indicating no oligomannose structures were present. Digestion with protein *N*-glycanase resulted in a shift from 75 to 50 kDa consistent with the presence of 7 *N*-glycans (Fig 10, *panel A*). The decrease in intensity upon Western blot analysis reflects increased sensitivity to degradation by plasma proteases following removal of the *N*-glycans. The properties of PSG23 summarized in Fig. 10 suggest that the PSGs produced during pregnancy bear glycans extensively modified with the Lewis^X structure Galβ1,4[Fucα1,3]GlcNAc that cannot accept the addition of sialic acid. This glycan would thus remain uncapped, ensuring its clearance by the ASGR when released into the circulation in mice expressing a full complement of the ASGR and promoting a highly localized site of action for PSG23 at the fetoplacental unit.

Additional glycoproteins were elevated in the plasma of *Asgr2*$^{-/-}$*Mrc1*$^{-/-}$ mice, including coagulation factors, collagens, lysosomal enzymes, and others. Eight different collagen α chains were elevated in the plasma of *Asgr2*$^{-/-}$*Mrc1*$^{-/-}$ (Table 1). The fibronectin type II domain of the ManR binds collagen (50), and two previous studies have also implicated the ManR in turnover of collagen *in vivo* (51, 52). For some proteins, the number of spectra obtained for elevated proteins in the double knock-out mice was not sufficient to be considered significant; *i.e.* <5, even though no spectra were obtained for those same proteins from WT plasma. This was true for lysosomal enzymes that have previously been reported to be elevated in *Mrc1*$^{-/-}$ mice (21) and for a number of coagulation factors. Thus, even when their levels were actually elevated, many proteins were not present in sufficient quantity to provide >5 spectra unless enriched to an even greater extent than was done for these studies. The number and fold elevation for circulating glycoproteins due to ablation of both the Man and the ASGR may thus be considerably greater than is indicated by the results in Table 1 and supplemental Table I.

The priapism seen in male *Asgr2*$^{-/-}$*Mrc1*$^{-/-}$ mice as a result of thrombosis of the penile vein could result from increased levels of certain coagulation factors; for example, vWF has previously been reported to be elevated in *Asgr2*$^{-/-}$ mice (16). We confirmed that vWF levels were elevated in *Asgr2*$^{-/-}$*Mrc1*$^{-/-}$

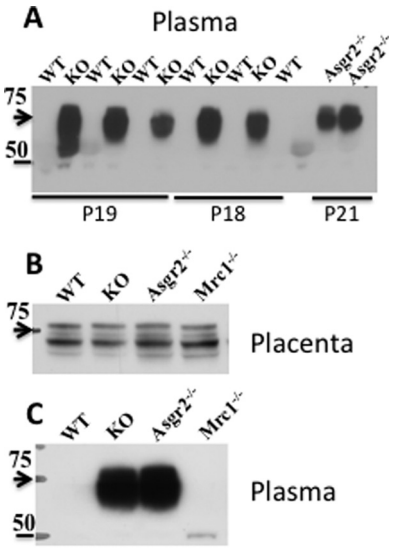

FIGURE 9. **PSG23 is elevated during pregnancy in *Asgr2*$^{-/-}$ *Mrc1*$^{-/-}$ and *Asgr2*$^{-/-}$ mice.** *Panel A,* plasma proteins, 25 μg/lane, from pregnant mice on day 18 (*P18*), day 19 (*P19*), and day 21 (*P21*) were subject to SDS-PAGE using 4–14% gradient gels under reducing conditions. The proteins were electrophoretically transferred to PVDF membranes and subject to Western blot analysis using rat anti-mouse PSG23. Lanes labeled *WT* were from wild type mice; lanes labeled *KO* were from *Asgr2*$^{-/-}$ *Mrc1*$^{-/-}$ double knock-out mice; and lanes labeled *Asgr2*$^{-/-}$ or Mrc*1*$^{-/-}$ were from single *Asgr2*$^{-/-}$ or *Mrc1*$^{-/-}$ knockouts, respectively. Staining of the PVDF following Western blot analysis demonstrated that protein loads were equal. *Panel B,* placenta proteins from day 18 of pregnancy were solubilized using T-PER (Pierce) and 25 μg of protein per lane was subject to SDS-PAGE using 4–14% gradient gels under reducing conditions. The proteins were electrophoretically transferred to PVDF membranes and subjected to Western blot analysis using rat anti-mouse PSG23. *Panel C,* plasma from the mice analyzed in *panel B* was examined by SDS-PAGE followed by Western blot using rat anti-mouse PSG23. *Arrowheads* indicate the location of a 75-kDa standard and the *bar* a 50-kDa standard.

mice via Western blot analysis and by immunoassay (Fig. 11). vWF was elevated in male mice, in both those that did and those that did not exhibit priapism (Fig. 11, *panel C*). Comparing the levels of circulating vWF in pregnant and non-pregnant female *Asgr2*$^{-/-}$*Mrc1*$^{-/-}$ mice revealed that the level of elevation and fraction of mice that had elevated levels was greater for pregnant than non-pregnant mice (Fig. 11, *panels B* and *C*). In contrast, there was no significant difference in vWF levels among pregnant and non-pregnant WT mice. In addition to vWF, coagulation Factor V was elevated 2.2-fold, and Factor XIIIA was elevated 6.8-fold in *Asgr2*$^{-/-}$*Mrc1*$^{-/-}$ pregnant mice (Table 1 and supplemental Table I). Elevated levels of vWF, Factor V, Factor XIIIA, transforming growth factor β_1-induced protein ig-h3 (TGFBIp/β Ig-h3), and a number of platelet glycoproteins suggest a generalized hypercoagulable state in double knock-out mice that could increase the probability of penile vein thrombosis in male mice during the stasis that occurs during erection.

Discussion

Ever since we characterized the unique *N*-glycans shown in Fig. 1 that terminate with β1,4-linked GalNAc-4-SO_4 on the glycoprotein hormone LH (37–40), we have sought to understand the biological function of these structures. Using genetically manipulated mice, we here demonstrate that clearance of endogenous LH is mediated by the ManR. In earlier studies, we demonstrated that LH and other glycoproteins bearing terminal β1,4-linked GalNAc-4-SO_4 are rapidly removed from the circulation by a receptor expressed by SECs that we identified as a dimeric form of the ManR (1, 22–24). Terminal GalNAc-4-SO_4 is bound by the cysteine-rich domain located at the N terminus of the ManR, and the bound glycoprotein is rapidly internalized (25, 26). We proposed that rapid clearance of LH by the ManR is required to generate the episodic rise and fall of LH seen *in vivo* following its regulated release from the pituitary that is required for optimal production of estrogen in the ovary.

We provided support for this proposed role for the ManR by ablating GalNAc-4-ST1, the sulfotransferase that mediates sulfate addition to β1,4-linked GalNAc on *N*-linked glycans (Fig. 1). In the absence of GalNAc-4-ST1 activity, the SO_4 on GalNAc was replaced by α2,6-linked sialic acid. The half-life of endogenous LH in *GalNAc-4-ST1* knock-out mice bearing this modified glycan structure was thereby increased, resulting in increased LH and estrogen/testosterone levels, premature sexual maturation, and enlarged uteri/seminal vesicles. These phenotypic alterations clearly supported the importance of pituitary glycoprotein hormone clearance on the basis of GalNAc-4-SO_4 (32). More recently, we reported that levels of ManR expression during pregnancy are regulated by progesterone, rising to maximum levels by 17 d.p.c. before beginning to decline. Furthermore, *Mrc1*$^{-/-}$ mice lose the ability to rapidly remove recombinant PSG23 bearing *N*-glycans terminating with GalNAc-4-SO_4 from the circulation (9).

Our current demonstration that clearance rates are prolonged for endogenous LH in both *Asgr2*$^{-/-}$*Mrc1*$^{-/-}$ and *Mrc1*$^{-/-}$ mice but not in *Asgr2*$^{-/-}$ mice, compared with WT mice, establishes that the ManR regulates the clearance rate for endogenous LH on the basis of its sulfate *N*-linked glycans. Like *GalNAc-4-ST1*$^{-/-}$ mice (32), *Mrc1*$^{-/-}$ male mice display increased levels of circulating LH and testosterone and enlarged seminal vesicles, a biological indicator of enhanced testosterone levels. Thus, the prolonged half-life seen for endogenous LH in *Mrc1*$^{-/-}$ male mice results in physiological changes that are similar to those seen in *GalNAc-4-ST1*$^{-/-}$ mice, further demonstrating the importance of the ManR in regulating LH function.

The ASGR mediates the rapid clearance of glycoproteins bearing glycans with terminal Gal or GalNAc (Fig. 1); however, the presence of SO_4 on the GalNAc of LH glycans prevents recognition by the ASGR. Thus, endogenous LH is cleared normally in *Asgr2*$^{-/-}$ mice. Nonetheless, expression of the ASGR, like that of the ManR, is regulated during pregnancy by progesterone (9), suggesting it may have a role during pregnancy. Remarkably, in the absence of clearance of ASGR-recognized structures in *Asgr2*$^{-/-}$ male mice, circulating levels of LH and testosterone are elevated, and seminal vesicle size is increased. Therefore, the ASGR contributes to the regulation of LH levels and as a consequence to testosterone levels *in vivo*. Male *Asgr2*$^{-/-}$ mice were fertile and did not display an obvious functional phenotype.

In contrast to male *Asgr2*$^{-/-}$ mice, female *Asgr2*$^{-/-}$ mice had a spontaneous functional phenotype comprising altered parameters of reproduction. Thirty five percent of female *Asgr2*$^{-/-}$ mice did not initiate parturition the evening of

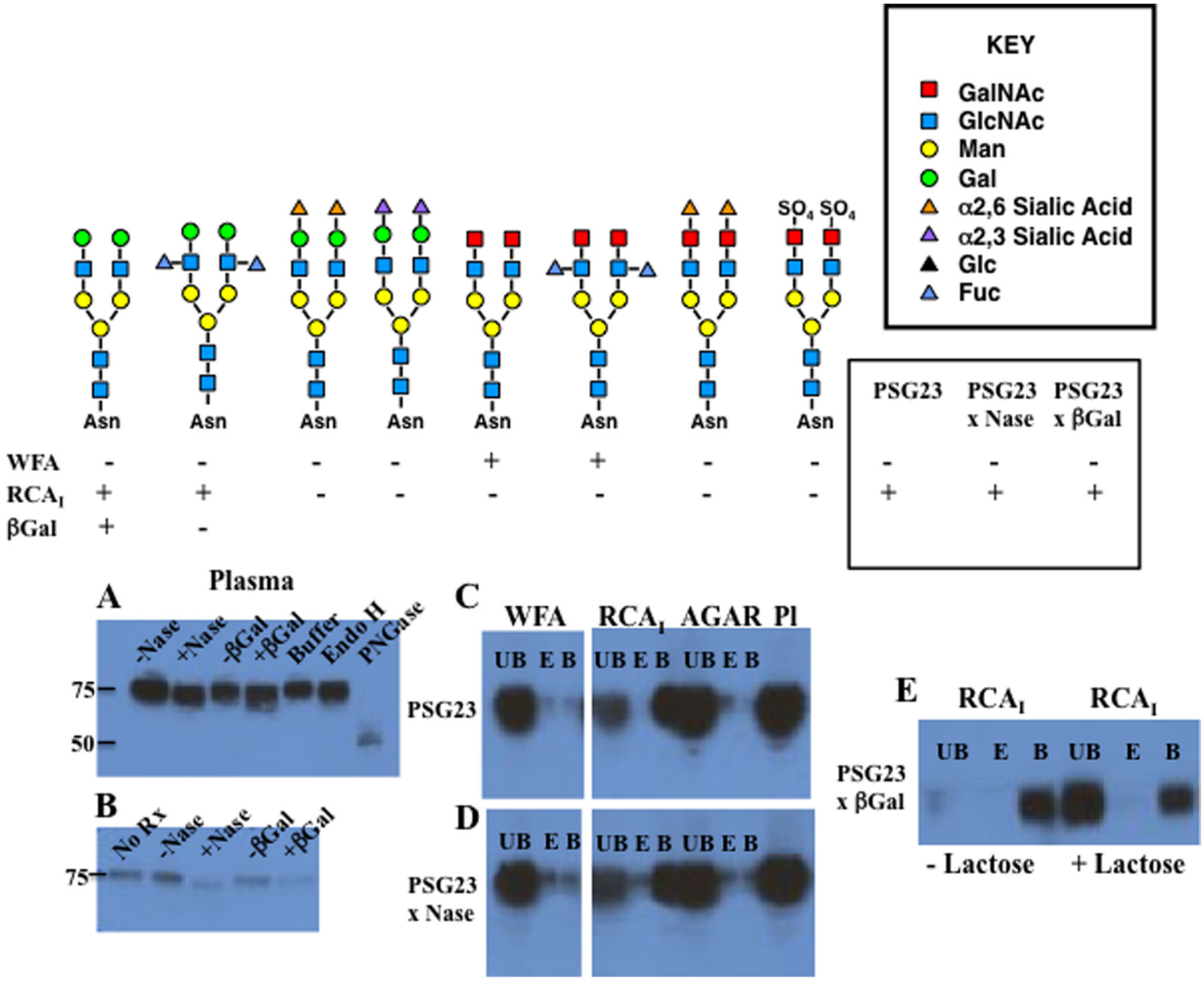

FIGURE 10. **Characteristics of PSG23 glycans from circulating PSG23 in *Asgr2*$^{-/-}$ *Mrc1*$^{-/-}$ mice.** *Left, top,* schematic of glycan structures that we generated on recombinant PSG23. *Left, bottom,* behavior of each version of PSG23 bearing the illustrated glycan structure, when incubated with immobilized WFA or RCA$_I$ is denoted as bound (+) or unbound (−). *Right, upper box,* key to glycan structure components shown at *left*. *Right, lower box,* behavior of PSG23 in plasma from *Asgr2*$^{-/-}$ *Mrc1*$^{-/-}$ mice. *Panels A* and *B*, plasma containing endogenous PSG23 was incubated in buffer (−) or digested (+) with neuraminidase (*Nase*), diplococcal β-galactosidase (*βGal*) with the specificity indicated, endoglycosidase H (*Endo H*), or protein *N*-glycanase (*PNGase*). Western blot analysis using anti-PSG23 following SDS-PAGE is shown. The location of 75- and 50-kDa standards is indicated. *Panel C,* plasma containing PSG23. *Panel D,* plasma containing PSG23 digested with neuraminidase was incubated with immobilized WFA, RCA$_I$, or unsubstituted agarose (*AGAR*). Aliquots of the unbound fraction (*UB*), the material eluted with GalNAc and lactose, respectively (*panel E*), and of material eluted by boiling the immobilized lectin in SDS-PAGE loading buffer (*panel B*) were subjected to Western blot analysis. *Pl* indicates an aliquot of plasma equal to that of the *UB*, *E*, and *B* fractions examined. *Panel E,* following digestion with diplococcal β-galactosidase (*βGal*) plasma was incubated the immobilized RCA$_I$-agarose in the absence (−) or presence (+) of lactose. The UB, E, and B fractions were analyzed by Western blotting with anti-PSG23 after SDS-PAGE. The plasma containing endogenous PSG23 was incubated with immobilized WFA or RCA$_I$, and the amount of PSG23 present in the UB, E, and B fractions were determined by Western blot analysis following SDS-PAGE. PSG23 was also digested with neuraminidase (*x Nase*) or neuraminidase followed by diplococcal β-galactosidase (*x βGal*) with the specificity indicated, prior to incubation with immobilized lectins. The properties of the PSG23 in the plasma from *Asgr2*$^{-/-}$ *Mrc1*$^{-/-}$ mice suggests that the predominant glycan structure on PSG23 is the Lewis^x structure shown.

d.p.c.19 and expired attempting to deliver post-mature pups. The fraction of mice unable to initiate parturition the evening of d.p.c.19 increased to >61% in *Asgr2*$^{-/-}$*Mrc1*$^{-/-}$ female mice. Thus, the inability to initiate parturition reflects primarily the lack of circulating glycoprotein clearance by the ASGR and is amplified by the additional of loss of clearance by the ManR.

Because clearance by both the ManR and the ASGR has an impact on LH levels, and expression of both receptors is regulated by progesterone over the course of pregnancy, the phenotype of *Asgr2*$^{-/-}$*Mrc1*$^{-/-}$ mice indicates that the ASGR and the ManR together play a critical role in regulating the initiation of parturition. Falling levels of progesterone contribute to the initiation of parturition in mice. RU486, a progesterone homologue that acts as a progesterone receptor antagonist and interferes with endogenous progesterone action, will induce premature parturition in mice. RU486 induced parturition in both WT and *Mrc1*$^{-/-}$ mice. In contrast, RU486 was not effective in initiating parturition in *Asgr2*$^{-/-}$*Mrc1*$^{-/-}$ mice and was only partially effective in *Asgr2*$^{-/-}$ mice. The resistance to RU486-induced parturition suggested that abnormal progesterone regulation alone was not the basis for the inability to initiate parturition at the proper time. The absence of pubic symphysis

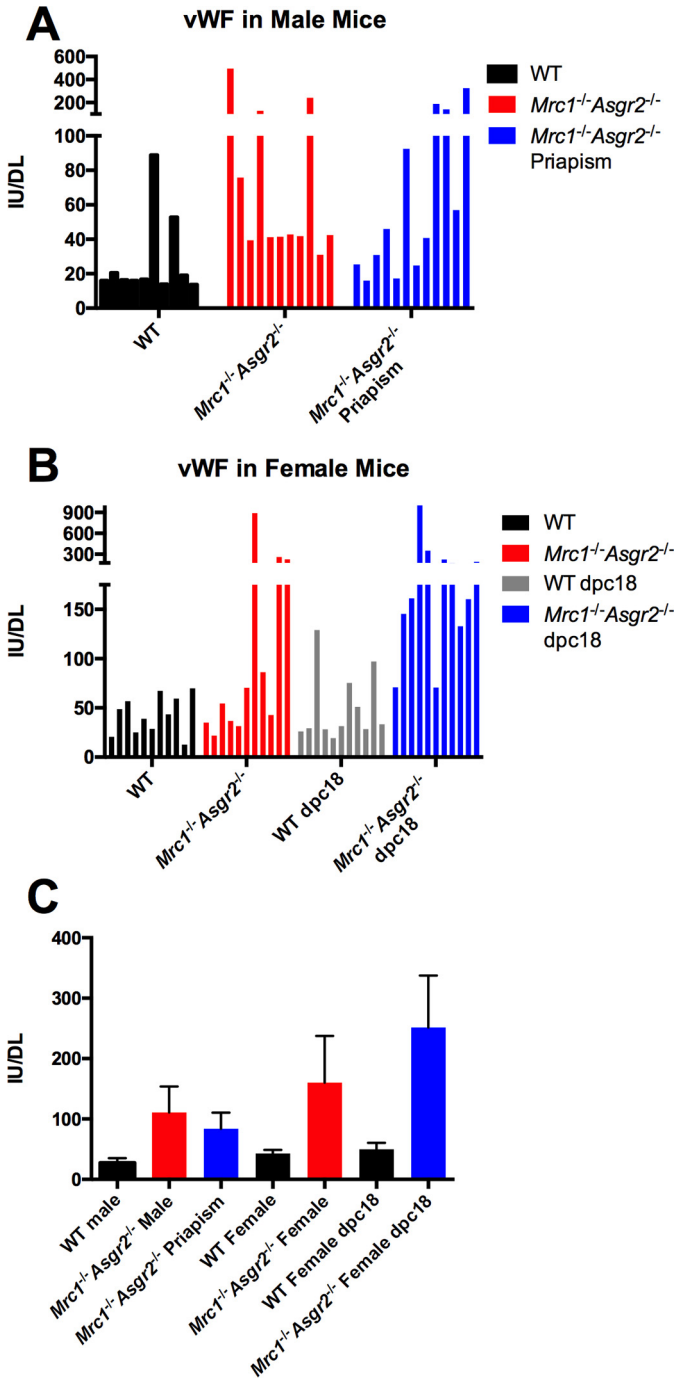

FIGURE 11. **von Willebrand factor is elevated in *Asgr2*$^{-/-}$ *Mrc1*$^{-/-}$ mice.** Plasma was obtained from WT male mice, *Asgr2*$^{-/-}$ *Mrc1*$^{-/-}$ male mice with and without priapism, WT female mice, *Asgr2*$^{-/-}$ *Mrc1*$^{-/-}$ female mice, WT pregnant female mice on P18, and pregnant *Asgr2*$^{-/-}$ *Mrc1*$^{-/-}$ female mice on P18 ($n = 11$ for each group). The amount of vWF was determined by ELISA as described. *Panel A* shows the values for individual male mice and *panel B* for individual female mice (70, 71). *Panel C* shows the mean and S.E. for each group. *p* values were determined using Mann-Whitney *t* test as follows: WT male *versus* *Asgr2*$^{-/-}$ *Mrc1*$^{-/-}$ male without priapism $p = 0.004$; WT male *versus* *Asgr2*$^{-/-}$ *Mrc1*$^{-/-}$ male with priapism $p = 0.013$; *Asgr2*$^{-/-}$ *Mrc1*$^{-/-}$ male with priapism *versus* without priapism $p = 0.41$; WT *versus* *Asgr2*$^{-/-}$ *Mrc1*$^{-/-}$ non-pregnant female $p = 0.19$; WT *versus* *Asgr2*$^{-/-}$ *Mrc1*$^{-/-}$ pregnant female on P18 $p = 0.0001$; and WT *versus* *Asgr2*$^{-/-}$ *Mrc1*$^{-/-}$ pregnant females on P18 = 0.047.

widening also suggested that multiple aspects of the process leading to parturition were abnormal in *Asgr2*$^{-/-}$*Mrc1*$^{-/-}$ mice.

The changes seen in *Mrc1*$^{-/-}$, *Asgr2*$^{-/-}$, and *Mrc1*$^{-/-}$ *Asgr2*$^{-/-}$ mice indicate that both the ManR and the ASGR contribute to regulation of the hypothalamus-pituitary-gonad axis. The elevated levels of LH and testosterone seen in *Asgr2*$^{-/-}$ mice suggest that a glycoprotein bearing a specific structure that would cause it to normally be cleared from the circulation by the ASGR acts as a positive regulator of LH levels *in vivo*. Testosterone and estrogen are negative regulators of LH levels. In contrast to testosterone and estrogen, this as yet unidentified glycoprotein cleared by the ASGR stimulates LH production. Our findings point to both positive and negative regulation of LH production and release by the pituitary on the basis of glycan structures. The increase in LH and testosterone seen in *Asgr2*$^{-/-}$*Mrc1*$^{-/-}$ mice was not greater than that seen in either *Asgr2*$^{-/-}$ or *Mrc1*$^{-/-}$ mice, suggesting that the inhibitory feedback effect of testosterone on LH production and release may dominate over positive regulation mediated via the unknown glycoprotein cleared by the ASGR. The decrease in LHβ mRNA levels seen in the pituitaries of *Asgr2*$^{-/-}$*Mrc1*$^{-/-}$ mice, as compared with the increases seen in both *Asgr2*$^{-/-}$ and *Mrc1*$^{-/-}$ mice (Fig. 6), could also reflect dominance of negative regulation by testosterone. We would not have been able to identify a role for a positive glycoprotein regulator of LH levels without the double knock-out of both the ManR and the ASGR.

The marked elevation of steady state transcript levels for 20αHSD, StAR, activin, inhibin, and LHR in the testis of *Asgr2*$^{-/-}$*Mrc1*$^{-/-}$ mice, as compared with either *Asgr2*$^{-/-}$ or *Mrc1*$^{-/-}$ mice, provides further evidence that two different forms of regulation are being exerted by the ManR and ASGR. The >10-fold elevation of 20αHSD transcript in the testis of *Asgr2*$^{-/-}$*Mrc1*$^{-/-}$ mice may serve to mute elevation of testosterone that would otherwise be even greater, because the progesterone is being converted to an inactive precursor. We have shown that ASGR expression is regulated by progesterone in pregnant mice and is maximal around 17 d.p.c. of pregnancy (9). Lack of clearance of glycans recognized by the ASGR in both *Asgr2*$^{-/-}$ and *Asgr2*$^{-/-}$*Mrc1*$^{-/-}$ mice at this point in pregnancy may disrupt the regulation of estrogen and progesterone levels critical for the initiation of parturition. This disruption would be further amplified by a lack of LH clearance by the ManR, potentially accounting for greater penetrance of the inability to initiate parturition in *Asgr2*$^{-/-}$*Mrc1*$^{-/-}$ mice as compared with *Asgr2*$^{-/-}$ mice. Additional glycoproteins exerting a direct effect on initiating parturition may also be elevated in the absence of clearance by the ASGR.

The remarkable numbers and types of glycoproteins elevated in the blood of pregnant *Asgr2*$^{-/-}$*Mrc1*$^{-/-}$ mice indicate that the ASGR and the ManR together regulate the circulating levels of many different glycoproteins. Certain glycoproteins that are known to be elevated in *Mrc1*$^{-/-}$ mice, for example many lysosomal enzymes (21), were not detected by our mass spectrometry strategy, most likely because they remain below the level required for detection. As a consequence, the list of glycoproteins whose concentration is regulated by the ASGR and/or the ManR may be considerably larger than that indicated in supplemental Table I. Because of the massive levels of ASGR and ManR expressed in the liver and their rapid rates of endocytosis and recycling to the cell surface, both receptors can reduce the

circulating quantities of glycoproteins that each recognizes to undetectable levels in a single pass through the liver.

PSG23 is illustrative of the capacity of the ASGR for clearance of circulating glycoproteins. In the absence of clearance by the ASGR, PSG23 reaches circulating levels of 10 mg/ml, yet it occurs at <50 ng/ml in WT mice. PSG23 is only one member of a family of multiple PSGs as well as other glycoproteins that are elevated in the absence of glycan-directed clearance by the ASGR. Thus, the capacity of the ASGR receptor to clear glycoproteins from the blood is truly remarkable.

Elevation of PSG23 and other PSGs was one of the most striking changes associated with the absence of clearance by the ASGR. The family of 17 *psg* gene products in mice is expressed by trophoblast giant cells and spongiotrophoblasts in the placenta over the course of pregnancy (33, 34, 42). The PSGs are extensively modified with *N*-glycans. PSG23 induces transforming growth factor β_1 (TGFβ_1) by macrophages, inhibits the interaction of platelets with fibrinogen, and induces endothelial tube formation *in vitro* (53), likely playing a role in vascular remodeling and immune regulation at the fetus-placenta interface (54–56). Remarkably, a target of the TGFβ_1 pathway, namely TGFBIp/β Ig-h3, is elevated 12-fold in the circulation of pregnant *Asgr2*$^{-/-}$*Mrc1*$^{-/-}$ mice (see Table 1). This suggests that PSG23 may be driving elevated levels of transforming growth factor β_1 in pregnant *Asgr2*$^{-/-}$*Mrc1*$^{-/-}$. Although characteristic of pregnancy, the precise function of PSG23 and the other murine PSGs *in vivo* remains unknown. The fact that PSGs are reduced to undetectable levels in WT mice suggests that their function *in vivo* is localized to the fetus-placenta interface, as they are rapidly cleared when they enter the blood.

Thrombosis of the penile vein and the resulting priapism seen in 25% of *Asgr2*$^{-/-}$*Mrc1*$^{-/-}$ mice indicated imbalances in coagulation. The coagulation factors vWF, Factor XIIIA, and Factor V, along with a number of platelet proteins, were among the circulating proteins elevated in *Asgr2*$^{-/-}$*Mrc1*$^{-/-}$ mice (Table 1 and supplemental Table I). vWF has previously been reported by Marth and co-workers (16) to be elevated in *Asgr2*$^{-/-}$ mice. We found that vWF was elevated in double knock-out males with and without priapism as well as in double knock-out females. The range of values seen for elevated vWF among individual animals was large (Fig. 11). vWF, stored in Weibel-Palade bodies of the endothelial cell, is released in response to endothelial cell injury and initiates coagulation by binding to exposed collagen (57). The markedly elevated levels of vWF seen among individual mice may reflect regulated release due to recent endothelial injury. It is possible that a large fraction of the vWF in Weibel-Palade bodies bears glycans that are normally recognized by the ASGR, causing this component of the vWF pool to be rapidly cleared in WT mice so as to limit coagulation to the site of release. The vWF remaining in the plasma of WT animals would in this case represent a fraction of material that is not rapidly cleared, potentially accounting for the long half-life that has been reported for vWF isolated from plasma (58, 59). Because vWF was elevated in males with and without priapism, it is not likely to alone account for the thrombosis of the penile vein.

Coagulation Factor V in humans and TGFBIp/β Ig-h3 in mice are associated with pulmonary embolism due to thrombus formation (60–63) and are elevated in plasma from *Asgr2*$^{-/-}$*Mrc1*$^{-/-}$ pregnant female mice (Table 1 and supplemental Table I). Following its activation, Factor V in humans accelerates thrombus formation during the conversion of prothrombin to thrombin. Activated Factor V is in turn inactivated by a serine protease termed activated protein C. A human mutant form of Factor V, Factor V Leiden, is resistant to proteolytic inactivation by activated protein C, resulting in increased amounts of circulating activated Factor V Leiden and an increased risk of venous thrombosis (61–63). Similarly increased levels of activated Factor V in *Asgr2*$^{-/-}$*Mrc1*$^{-/-}$ male mice, reflecting a lack of clearance of this coagulation factor, could result in thrombosis of the penile vein due to venous stasis during erection. TGFBIp/β Ig-h3, a matrix protein that may promote platelet adhesion, is also associated with thrombus formation (60). Transgenic mice with a 1.7-fold increase in circulating TGFBIp/β Ig-h3 are more susceptible to formation of collagen-induced pulmonary emboli (60). Thus, elevated levels of Factor V and/or TGFBIp/β Ig-h3 may contribute to thrombus formation in the penile vein. Because priapism was only observed in *Asgr2*$^{-/-}$*Mrc1*$^{-/-}$ male mice, it would appear that proteins cleared by both receptors contribute to the increased risk of thrombosis in these mice.

Our studies here demonstrate that the ASGR and the ManR play a much broader role in regulation of the circulatory half-lives of a wide range of plasma glycoproteins than has previously been appreciated. The high expression levels of these receptors and their rapid rate of internalization, in combination with the large number of PCs and SECs that make up the liver, result in an enormous capacity for clearance of glycoproteins. Reducing the concentration of circulating glycoproteins bearing glycans recognized by the ASGR and the ManR to undetectable levels may serve to prevent harmful effects, for example from activated coagulation factors or lysosomal enzymes. The receptors also determine the circulatory half-life of other glycoproteins such as the glycoprotein hormone LH following its regulated release by cells in the pituitary (9, 23, 32). The ASGR and the ManR are multifunctional entities by virtue of the glycoproteins that they recognize and the manner in which they remove them from the circulation. The ASGR and the ManR play critical roles in reproduction by regulating hormonal levels. Defining precisely how they accomplish this will lead to new insights that may allow us to better predict and control the process of parturition and other aspects of reproduction. The translational implications of our work point toward future strategies to reduce risk factors associated with pregnancy such as an increased risk of thrombosis.

Experimental Procedures

Timed Mating—Mrc1$^{-/-}$*Asgr2*$^{-/-}$ knock-out mice were generated and maintained by mating *Mrc1*$^{-/-}$*Asgr2*$^{-/-}$ male mice with *Mrc1*$^{-/-}$*Asgr2*$^{-/+}$ female mice. Female mice mated overnight with male mice were examined the following morning for the presence of a vaginal plug; gestational age was designated as 0.5 d.p.c. for those mice with a vaginal plug. RU486 (mifepristone), a progesterone receptor antagonist (36), was used to induce preterm labor by injecting pregnant mice sub-

cutaneously (150 μg of mifepristone in 100 μl of corn oil containing 10% ethanol) on 15.5 d.p.c.

Serum Collection—Mice were anesthetized with ketamine (87 mg/kg) and xylazine (13 mg/kg) for terminal blood collection by cardiac puncture. Blood was allowed to clot for 60 min at 25 °C and then sedimented for 15 min at 25 °C by centrifugation. The serum was removed and stored at −80 °C until analysis.

Clearance of Endogenous LH—Male mice were castrated 5 days prior to examining the clearance of endogenous LH as described previously (32). A 2-cm ventral midline incision was made in the scrotum of mice anesthetized with ketamine (87 mg/kg) and xylazine (13.4 mg/kg). The tunica was pierced, and the testis was pushed out by gentle pressure. The spermatic artery was cauterized and the testis removed. The epididymis, deferential vessels, and ductus were replaced in the tunica. The incision was closed with wound clips.

Clearance studies were performed with anesthetized mice. Following collection of a baseline sample of 150 μl of blood, designated time 0, each mouse was injected intravenously with 10 μg of acyline (Woods Assay Inc., Portland, OR) via the lateral tail vein. Blood (150 μl) was drawn retro-orbitally at the times indicated. After each withdrawal, 200 μl of warm saline was injected into the peritoneum.

Hormone Assays—Quantitation of LH, FSH, and testosterone was performed by the University of Virginia Center for Research in Reproduction Ligand Assay and Analysis Core (Charlottesville, VA).

Histology—Mouse penile tissues were fixed in 10% buffered formalin overnight at room temperature, embedded in paraffin, and sectioned. For morphological studies, the slides were stained with hematoxylin and eosin.

Analysis of mRNA Expression by Real Time Quantitative PCR—Tissues were homogenized in TRIzol (Life Technologies, Inc.) according to the manufacturer's instructions. RNA purity and concentration were determined with Nanodrop 2000c (NanoDrop Products, Wilmington, DE). One microgram of total RNA was reverse-transcribed using Omniscript reverse transcriptase (Qiagen, Valencia, CA) in a volume of 20 μl using the protocol supplied by the manufacturer. For real time PCR, each reaction contained 9 μl of cDNA diluted 1:25 in diethyl pyrocarbonate-treated water, and 10 μl of TaqMan Universal Fast Master Mix (Applied Biosystems), 1 μl of primer mix, and primers were used to perform real time PCR in triplicate using a StepOnePlus (Applied Biosystems). Melting curve analysis was performed to confirm the absence of nonspecific product amplification for each primer set. For quantification, the $\Delta\Delta C_T$ method (64) was used to determine the relative expression between groups. The threshold cycle (C_T) was determined for genes of interest and the housekeeping gene *Hprt1*. The data were normalized by subtracting the C_T for each gene of interest from the C_T for *Hprt1* to determine the ΔC_T value. After this loading control correction, the relative expression levels of the genes of interest in an experimental sample was compared with that of calibrator sample by subtracting their ΔC_T values. In our experiments, we used a cDNA pool of all the samples as the calibrator. By using the same calibrator, the relative expression for every sample was calculated using the following formula: relative fold change $= 2^{-x}$, where x is the difference between the ΔC_T of the experimental sample and the calibrator sample.

Multiaffinity Fractionation (MAF) of Mouse Plasma—Four 75-μl aliquots of plasma from 18.5 d.p.c. WT and *Mrc1*$^{-/-}$ *Asgr2*$^{-/-}$ mice were pooled for analysis. Six highly abundant proteins were depleted from the pooled samples (albumin, IgG, IgA, haptoglobin, transferrin, and α-1-antitrypsin) by immunoaffinity chromatography (Agilent Technologies, Palo Alto, CA). MAF was performed on a BioCAD Vision Workstation, using a Cavro AFC 2000 autosampler/fraction collector. The affinity runs were monitored with a UV detector at 280 nm. For automated MAF, an equal volume of 2× TBS (20 mM Tris-HCl, 150 mM NaCl, pH 7.4) was added to each of the frozen plasma samples. After gentle inversion, each sample was filtered through a 0.45-μm filter unit (Millipore, Billerica, MA), and an 800-μl aliquot of the filtrate was diluted to 2100 μl with 1× TBS. The diluted samples were injected onto the affinity columns from an autosampler at 4 °C. Bound proteins were eluted from the column with 25 ml of 100 mM glycine buffer, pH 2.5, and discarded. The affinity column was then neutralized with 100 mM Tris-Cl, pH 8, and re-equilibrated with TBS, pH 7.4. The flow-through fraction was transferred to a concentrating device (Amicon Ultra-15, nominal molecular mass cutoff = 3 kDa) and centrifuged according to manufacturer's guidelines (4000 × *g*, 4 °C), reducing the volume to ~300 μl for subsequent analyses.

Analytical One-dimensional SDS-PAGE—The reproducibility of automated MAF of the plasma samples was initially evaluated using analytical SDS-PAGE. Protein concentrations of the concentrated depleted plasma samples were determined using the Advanced Protein Assay reagent (Cytoskeleton, Denver, CO) against a curve made with BSA standard solution (Pierce), measured at 590 nm. Aliquots of the concentrated samples, each containing 5 μg of protein (~10 μl), were diluted with 5 μl of 4× sample buffer (Bio-Rad) and 1 μl of 20× reductant (Bio-Rad), heated to 95 °C for 5 min, cooled to room temperature, centrifuged at 13,000 rpm for 30–60 s, and loaded with molecular weight markers (Bio-Rad Precision Plus Protein standards, catalogue no. 161-0363) onto 4–12% Criterion XT BisTris gels. Gels were run in MES buffer, monitored using the blue dye front, placed in fixative solution (10% methanol, 5% acetic acid) for 1 h, stained with SyproRuby (Invitrogen) for 2 h, destained (10% methanol, 5% acetic acid) for 30 min, and scanned on a Typhoon 9400 scanner (GE Healthcare, UK) using the following settings: 457 nm excitation, 610BP30 emission filter, and photomultiplier tube voltage adjusted to stay below saturation for the darkest band.

Preparation of Peptides from MAF Plasma—The concentrated unbound eluates from the multiaffinity columns were precipitated using the vendor protocol for the two-dimensional clean-up kit (GE Healthcare). Protein pellets were solubilized in 20 μl of Tris buffer (100 mM, pH 8.5) containing 8 M urea. Disulfide bonds were reduced with 1 mM tris(2-carboxyethyl) phosphine (bond breaker, 0.5 M solution, Thermo Fisher, Waltham, MA) at room temperature for 30 min. Cysteine alkylation was performed using 2.2 μl of 100 mM iodoacetamide for 30 min at room temperature while protected from light, and then quenched with 10 mM dithiothreitol at room temperature for 15 min. The reduced and alkylated protein samples (~30 μl)

were digested overnight at 37 °C in 8 M urea with 1 μg of endoproteinase Lys-C (2 μl of a 0.5 μg/μl stock; Roche Applied Science, Basel, Switzerland), then diluted 1:4 with 100 mM Tris, pH 8.5, incubated with trypsin (Sigma) (~1:4 enzyme ratio) for 24 h at 37 °C, and acidified with aqueous 5% formic acid (3.3 μl) (Fluka, St. Louis, MO; catalogue no. 56302). Peptides were extracted with Nutip carbon tips (Glygen, Columbia, MD; catalogue no. NT3CAR) that were preconditioned by repetitive pipetting with 25 μl (three times) of the peptide elution solvent (60% acetonitrile in 1% formic acid) followed by equilibration with 10 washes (25 μl) of extraction solvent (1% formic acid). Samples were loaded with 50 pipetting cycles. The tips were then washed four times with extraction solution. The peptides were recovered by 20 pipetting cycles with 25 μl of elution solution and followed by four washes (20 μl each) of elution solution. The extraction and wash solutions were combined in an autosampler vial (SunSri, Rockwood, TN) and dried in a SpeedVac (Thermo Scientific Savant). AS2 autosampler vial caps were from National Scientific (Rockwood, TN).

Nano-liquid Chromatography-Mass Spectrometry (LC-MS)—A two-dimensional Plus LC (Eksigent, Dublin, CA) with a Nanoflex module and an AS2 autosampler were coupled to a TripleTOF 5600 Plus mass spectrometer (AB SCIEX). The two-dimensional LC system was configured to load samples in tandem. The CHiPLC columns (ChromXP C_{18} 200 μm × 15 cm; particle size 3 μm, 120 Å) were equilibrated in 1% aqueous formic acid (solvent A). Organic gradients were produced by increasing the proportion of solvent B (1% formic acid in acetonitrile): 0 min, 98% solvent A, 2% solvent B; 5 min, 98% A, 2% B; 400 min, 65% A, 35% B; 450 min, 20% A, 80% B; ending at 60 min. Initial chromatographic conditions were restored in 5 min and maintained for 20 min. The samples were loaded in a volume of 10 μl at a flow rate of 1.5 μl/min followed by gradient elution of peptides at a flow rate of 800 nl/min.

MS data acquisition was performed with a TripleTOF 5600 Plus (AB SCIEX) mass spectrometer interfaced to the nanochromatography with a Digital Picoview nanospray source (New Objectives) via a 10-μm Silica PicoTip emitter (New Objectives) and operated with a resolution of $>30{,}000_{\mathrm{fwhm}}$ for TOF-MS scans. Data were acquired with the ion spray voltage at 2.9 kV, curtain gas at 10 p.s.i., nebulizer gas at 14 p.s.i., and the interface heater temperature of 175 °C. For data-dependent acquisition, survey scans were acquired in 250 ms; from these, 50 product ion scans were selected for MS2 acquisition with a dwell time of 20 ms. Four time bins were summed for each scan at a frequency of 15.4 kHz (through monitoring of the 40 GHz multichannel TDC detector with four-anode/channel detection). A rolling collision energy (CE) was applied to all precursor ions for collision-induced dissociation using Equation 1,

$$\mathrm{CE} = \mathrm{slope} \cdot m/z + \mathrm{intercept} \qquad \text{(Eq. 1)}$$

where the slope for all charge states above +2 is 0.0625, and the intercept is −3, −5, and −6 for +2, +3, and +4, respectively.

MS Data Processing and Protein Quantification—Data were processed using the AB SCIEX MS Data Converter version 1.3 (AB SCIEX), converting the raw data files (*.wiff) to mgf files for protein database searching. A copy of the Uniprot mouse reference database (downloaded Oct. 8, 2013, containing 43,296 entries) was used to perform a MASCOT (version 2.5.1) decoy search allowing for up to four missed cleavages. The parent and product mass search tolerances were set at 25 ppm and 0.1 Da, respectively. Carbamidomethyl was set as a fixed modification for cysteine residues, and methionine residue oxidation was allowed as a variable modification. The protein database searches were analyzed using Scaffold (version 4.4.8), and proteins were identified using the Protein Prophet algorithm (65, 66) with protein and peptide thresholds at 1% and 0.1% false discovery rate, respectively. Quantification of relative protein abundance was performed using spectral counting (67, 68) with *p* values generated in Scaffold (version 4.0) using a Fisher's exact test (69). Proteins with at least five or greater spectral counts were used to quantify changes in protein abundances.

Plasma vWF Quantitation—Plasma levels of vWF were determined as described previously (70, 71).

Generation of Rat Anti-PSG23 Antibody—PSG23 consisting of the N-terminal domain and the A-domain (PSG23N1A) followed by the HRV 3C protease recognition sequence, Leu-Glu-Val-Leu-Phe-Gln-Gly-Pro, a His_6, and a FLAG tag was generated and purified as described previously (54). To generate the anti-PSG23 antibody, rats were immunized with PSG23N1A following in-column cleavage of the tags. Briefly, PSG23N1A His FLAG purified with an anti-FLAG M2-agarose column (Sigma) was equilibrated in protease (HRV 3C) reaction buffer and applied to a HisTrap column (GE Healthcare). The column was washed with 5 column volumes of reaction buffer followed by the addition of 1 unit of HRV 3C protease (Pierce) per 100 μg of PSG23N1A and incubated overnight. The cleaved protein was eluted from the column, concentrated, buffer-exchanged with PBS, and used as the immunogen.

Author Contributions—J. U. B. designed the studies and wrote the manuscript. Y. M. and D. F. helped design the studies, performed the analyses, and wrote sections of the manuscript. M. C. performed the PSG23 analyses and analyzed the pubic symphyses. L. S. performed the initial studies with RU486. G. D. prepared the antibodies directed as PSG23 and provided standards for quantitative Western blottings. R. R. T. performed the mass spectral studies.

Acknowledgments—We thank Petra Erdmann-Gilmore and Anne Kettler for expert technical assistance in the generation of the proteomics data, and Jim Malone for assistance with data analysis and manuscript preparation. We thank Mary C. Beranek for preparation of constructs and Karl Desch and David Ginsburg (University of Michigan) for performing von Willebrand factor quantitations. We also thank Nancy L. Baenziger for critical reading of the manuscript and helpful suggestions.

References

1. Fiete, D., Srivastava, V., Hindsgaul, O., and Baenziger, J. U. (1991) A hepatic reticuloendothelial cell receptor specific for SO4–4GalNAc β1,4GlcNAc β1,2Manα that mediates rapid clearance of lutropin. *Cell* **67,** 1103–1110
2. Maynard, Y., and Baenziger, J. U. (1981) Oligosaccharide specific endocytosis by isolated rat hepatic reticuloendothelial cells. *J. Biol. Chem.* **256,** 8063–8068
3. Ashwell, G., and Harford, J. (1982) Carbohydrate-specific receptors of the liver. *Annu. Rev. Biochem.* **51,** 531–554

4. Stockert, R. J. (1995) The asialoglycoprotein receptor: relationships between structure, function, and expression. *Physiol. Rev.* **75,** 591–609
5. Hubbard, A. L., Wilson, G., Ashwell, G., and Stukenbrok, H. (1979) An electron microscope autoradiographic study of the carbohydrate recognition systems in rat liver. I. Distribution of ^{125}I-ligands among the liver cell types. *J. Cell Biol.* **83,** 47–64
6. Weis, W. I., and Drickamer, K. (1996) Structural basis of lectin-carbohydrate recognition. *Annu. Rev. Biochem.* **65,** 441–473
7. Morell, A. G., Gregoriadis, G., Scheinberg, I. H., Hickman, J., and Ashwell, G. (1971) The role of sialic acid in determining the survival of glycoproteins in the circulation. *J. Biol. Chem.* **246,** 1461–1467
8. Hudgin, R. L., Pricer, W. E., Jr., Ashwell, G., Stockert, R. J., and Morell, A. G. (1974) The isolation and properties of a rabbit liver binding protein specific for asialoglycoproteins. *J. Biol. Chem.* **249,** 5536–5543
9. Mi, Y., Lin, A., Fiete, D., Steirer, L., and Baenziger, J. U. (2014) Modulation of mannose and asialoglycoprotein receptor expression determines glycoprotein hormone half-life at critical points in the reproductive cycle. *J. Biol. Chem.* **289,** 12157–12167
10. Park, E. I., Mi, Y., Unverzagt, C., Gabius, H. J., and Baenziger, J. U. (2005) The asialoglycoprotein receptor clears glycoconjugates terminating with sialic acid α2,6GalNAc. *Proc. Natl. Acad. Sci. U.S.A.* **102,** 17125–17129
11. Park, E. I., and Baenziger, J. U. (2004) Closely related mammals have distinct asialoglycoprotein receptor carbohydrate specificities. *J. Biol. Chem.* **279,** 40954–40959
12. Baenziger, J. U., and Fiete, D. (1980) Galactose and *N*-acetylgalactosamine-specific endocytosis of glycopeptides by isolated rat hepatocytes. *Cell* **22,** 611–620
13. Braun, J. R., Willnow, T. E., Ishibashi, S., Ashwell, G., and Herz, J. (1996) The major subunit of the asialoglycoprotein receptor is expressed on the hepatocellular surface in mice lacking the minor receptor subunit. *J. Biol. Chem.* **271,** 21160–21166
14. Ishibashi, S., Hammer, R. E., and Herz, J. (1994) Asialoglycoprotein receptor deficiency in mice lacking the minor receptor subunit. *J. Biol. Chem.* **269,** 27803–27806
15. Tozawa, R., Ishibashi, S., Osuga, J., Yamamoto, K., Yagyu, H., Ohashi, K., Tamura, Y., Yahagi, N., Iizuka, Y., Okazaki, H., Harada, K., Gotoda, T., Shimano, H., Kimura, S., Nagai, R., *et al.* (2001) Asialoglycoprotein receptor deficiency in mice lacking the major receptor subunit. Its obligate requirement for the stable expression of oligomeric receptor. *J. Biol. Chem.* **276,** 12624–12628
16. Grewal, P. K., Uchiyama, S., Ditto, D., Varki, N., Le, D. T., Nizet, V., and Marth, J. D. (2008) The Ashwell receptor mitigates the lethal coagulopathy of sepsis. *Nat. Med.* **14,** 648–655
17. Rumjantseva, V., Grewal, P. K., Wandall, H. H., Josefsson, E. C., Sørensen, A. L., Larson, G., Marth, J. D., Hartwig, J. H., and Hoffmeister, K. M. (2009) Dual roles for hepatic lectin receptors in the clearance of chilled platelets. *Nat. Med.* **15,** 1273–1280
18. Stahl, P., Six, H., Rodman, J. S., Schlesinger, P., Tulsiani, D. R., and Touster, O. (1976) Evidence for specific recognition sites mediating clearance of lysosomal enzymes *in vivo*. *Proc. Natl. Acad. Sci. U.S.A.* **73,** 4045–4049
19. Stahl, P. D., and Ezekowitz, R. A. (1998) The mannose receptor is a pattern recognition receptor involved in host defense. *Curr. Opin. Immunol.* **10,** 50–55
20. Taylor, P. R., Martinez-Pomares, L., Stacey, M., Lin, H. H., Brown, G. D., and Gordon, S. (2005) Macrophage receptors and immune recognition. *Annu. Rev. Immunol.* **23,** 901–944
21. Lee, S. J., Evers, S., Roeder, D., Parlow, A. F., Risteli, J., Risteli, L., Lee, Y. C., Feizi, T., Langen, H., and Nussenzweig, M. C. (2002) Mannose receptor-mediated regulation of serum glycoprotein homeostasis. *Science* **295,** 1898–1901
22. Roseman, D. S., and Baenziger, J. U. (2000) Molecular basis of lutropin recognition by the mannose/GalNAc-4-SO4 receptor. *Proc. Natl. Acad. Sci. U.S.A.* **97,** 9949–9954
23. Baenziger, J. U., Kumar, S., Brodbeck, R. M., Smith, P. L., and Beranek, M. C. (1992) Circulatory half-life but not interaction with the lutropin/chorionic gonadotropin receptor is modulated by sulfation of bovine lutropin oligosaccharides. *Proc. Natl. Acad. Sci. U.S.A.* **89,** 334–338
24. Fiete, D., and Baenziger, J. U. (1997) Isolation of the SO4-4-GalNAcβ1,4GlcNAcβ1,2Manα-specific receptor from rat liver. *J. Biol. Chem.* **272,** 14629–14637
25. Fiete, D. J., Beranek, M. C., and Baenziger, J. U. (1998) A cysteine-rich domain of the "mannose" receptor mediates GalNAc-4-SO4 binding. *Proc. Natl. Acad. Sci. U.S.A.* **95,** 2089–2093
26. Fiete, D., Beranek, M. C., and Baenziger, J. U. (1997) The macrophage/endothelial cell mannose receptor cDNA encodes a protein that binds oligosaccharides terminating with SO4–4-GalNAcβ1,4GlcNAcβ or Man at independent sites. *Proc. Natl. Acad. Sci. U.S.A.* **94,** 11256–11261
27. Taylor, M. E., and Drickamer, K. (1993) Structural requirements for high affinity binding of complex ligands by the macrophage mannose receptor. *J. Biol. Chem.* **268,** 399–404
28. Liu, Y., Chirino, A. J., Misulovin, Z., Leteux, C., Feizi, T., Nussenzweig, M. C., and Bjorkman, P. J. (2000) Crystal structure of the cysteine-rich domain of mannose receptor complexed with a sulfated carbohydrate ligand. *J. Exp. Med.* **191,** 1105–1116
29. Kang, H. G., Evers, M. R., Xia, G., Baenziger, J. U., and Schachner, M. (2001) Molecular cloning and expression of an *N*-acetylgalactosamine-4-*O*-sulfotransferase that transfers sulfate to terminal and non-terminal β1,4-linked N-acetylgalactosamine. *J. Biol. Chem.* **276,** 10861–10869
30. Xia, G., Evers, M. R., Kang, H. G., Schachner, M., and Baenziger, J. U. (2000) Molecular cloning and expression of the pituitary glycoprotein hormone *N*-acetylgalactosamine-4-*O*-sulfotransferase. *J. Biol. Chem.* **275,** 38402–38409
31. Smith, P. L., and Baenziger, J. U. (1990) Recognition by the glycoprotein hormone-specific *N*-acetylgalactosaminetransferase is independent of hormone native conformation. *Proc. Natl. Acad. Sci. U.S.A.* **87,** 7275–7279
32. Mi, Y., Fiete, D., and Baenziger, J. U. (2008) Ablation of GalNAc-4-sulfotransferase-1 enhances reproduction by altering the carbohydrate structures of luteinizing hormone in mice. *J. Clin. Invest.* **118,** 1815–1824
33. Zebhauser, R., Kammerer, R., Eisenried, A., McLellan, A., Moore, T., and Zimmermann, W. (2005) Identification of a novel group of evolutionarily conserved members within the rapidly diverging murine Cea family. *Genomics* **86,** 566–580
34. McLellan, A. S., Zimmermann, W., and Moore, T. (2005) Conservation of pregnancy-specific glycoprotein (PSG) N domains following independent expansions of the gene families in rodents and primates. *BMC Evol. Biol.* **5,** 39
35. Sherwood, O. D. (2004) Relaxin's physiological roles and other diverse actions. *Endocr. Rev.* **25,** 205–234
36. Piekorz, R. P., Gingras, S., Hoffmeyer, A., Ihle, J. N., and Weinstein, Y. (2005) Regulation of progesterone levels during pregnancy and parturition by signal transducer and activator of transcription 5 and 20α-hydroxysteroid dehydrogenase. *Mol. Endocrinol.* **19,** 431–440
37. Green, E. D., and Baenziger, J. U. (1988) Asparagine-linked oligosaccharides on lutropin, follitropin, and thyrotropin. I. Structural elucidation of the sulfated and sialylated oligosaccharides on bovine, ovine, and human pituitary glycoprotein hormones. *J. Biol. Chem.* **263,** 25–35
38. Green, E. D., and Baenziger, J. U. (1988) Asparagine-linked oligosaccharides on lutropin, follitropin, and thyrotropin. II. Distributions of sulfated and sialylated oligosaccharides on bovine, ovine, and human pituitary glycoprotein hormones. *J. Biol. Chem.* **263,** 36–44
39. Baenziger, J. U., and Green, E. D. (1988) Pituitary glycoprotein hormone oligosaccharides: structure, synthesis and function of the asparagine-linked oligosaccharides on lutropin, follitropin and thyrotropin. *Biochim. Biophys. Acta* **947,** 287–306
40. Green, E. D., van Halbeek, H., Boime, I., and Baenziger, J. U. (1985) Structural elucidation of the disulfated oligosaccharide from bovine lutropin. *J. Biol. Chem.* **260,** 15623–15630
41. Roseman, D. S., and Baenziger, J. U. (2001) The mannose/*N*-acetylgalactosamine-4-SO4 receptor displays greater specificity for multivalent than monovalent ligands. *J. Biol. Chem.* **276,** 17052–17057
42. McLellan, A. S., Fischer, B., Dveksler, G., Hori, T., Wynne, F., Ball, M., Okumura, K., Moore, T., and Zimmermann, W. (2005) Structure and evolution of the mouse pregnancy-specific glycoprotein (Psg) gene locus. *BMC Genomics* **6,** 4
43. Coombs, P. J., Taylor, M. E., and Drickamer, K. (2006) Two categories of

mammalian galactose-binding receptors distinguished by glycan array profiling. *Glycobiology* **16,** 1C–7C
44. Merkle, R. K., and Cummings, R. D. (1987) Lectin affinity chromatography of glycopeptides. *Methods Enzymol.* **138,** 232–259
45. Green, E. D., and Baenziger, J. U. (1989) Characterization of oligosaccharides by lectin affinity high-performance liquid chromatography. *Trends Biochem. Sci.* **14,** 168–172
46. Green, E. D., Brodbeck, R. M., and Baenziger, J. U. (1987) Lectin affinity high-performance liquid chromatography: interactions of *N*-glycanase-released oligosaccharides with leuko-agglutinating phytohemagglutinin, concanavalin A, *Datura stramonium* agglutinin, and Vicia villosa agglutinin. *Anal. Biochem.* **167,** 62–75
47. Green, E. D., Brodbeck, R. M., and Baenziger, J. U. (1987) Lectin affinity high-performance liquid chromatography. Interactions of *N*-glycanase-released oligosaccharides with *Ricinus communis* agglutinin I and *Ricinus communis* agglutinin II. *J. Biol. Chem.* **262,** 12030–12039
48. Mengeling, B. J., Smith, P. L., Stults, N. L., Smith, D. F., and Baenziger, J. U. (1991) A microplate assay for analysis of solution-phase glycosyltransferase reactions: determination of kinetic constants. *Anal. Biochem.* **199,** 286–292
49. Mandalasi, M., Dorabawila, N., Smith, D. F., Heimburg-Molinaro, J., Cummings, R. D., and Nyame, A. K. (2013) Development and characterization of a specific IgG monoclonal antibody toward the Lewis x antigen using splenocytes of *Schistosoma mansoni*-infected mice. *Glycobiology* **23,** 877–892
50. Napper, C. E., Drickamer, K., and Taylor, M. E. (2006) Collagen binding by the mannose receptor mediated through the fibronectin type II domain. *Biochem. J.* **395,** 579–586
51. Madsen, D. H., Leonard, D., Masedunskas, A., Moyer, A., Jürgensen, H. J., Peters, D. E., Amornphimoltham, P., Selvaraj, A., Yamada, S. S., Brenner, D. A., Burgdorf, S., Engelholm, L. H., Behrendt, N., Holmbeck, K., Weigert, R., *et al.* (2013) M2-like macrophages are responsible for collagen degradation through a mannose receptor-mediated pathway. *J. Cell Biol.* **202,** 951–966
52. Malovic, I., Sørensen, K. K., Elvevold, K. H., Nedredal, G. I., Paulsen, S., Erofeev, A. V., Smedsrød, B. H., and McCourt, P. A. (2007) The mannose receptor on murine liver sinusoidal endothelial cells is the main denatured collagen clearance receptor. *Hepatology* **45,** 1454–1461
53. Shanley, D. K., Kiely, P. A., Golla, K., Allen, S., Martin, K., O'Riordan, R. T., Ball, M., Aplin, J. D., Singer, B. B., Caplice, N., Moran, N., and Moore, T. (2013) Pregnancy-specific glycoproteins bind integrin αIIbβ3 and inhibit the platelet-fibrinogen interaction. *PLoS ONE* **8,** e57491
54. Wu, J. A., Johnson, B. L., Chen, Y., Ha, C. T., and Dveksler, G. S. (2008) Murine pregnancy-specific glycoprotein 23 induces the proangiogenic factors transforming-growth factor β1 and vascular endothelial growth factor a in cell types involved in vascular remodeling in pregnancy. *Biol. Reprod.* **79,** 1054–1061
55. Ha, C. T., Waterhouse, R., Warren, J., Zimmermann, W., and Dveksler, G. S. (2008) *N*-Glycosylation is required for binding of murine pregnancy-specific glycoproteins 17 and 19 to the receptor CD9. *Am. J. Reprod. Immunol.* **59,** 251–258
56. Snyder, S. K., Wessner, D. H., Wessells, J. L., Waterhouse, R. M., Wahl, L. M., Zimmermann, W., and Dveksler, G. S. (2001) Pregnancy-specific glycoproteins function as immunomodulators by inducing secretion of IL-10, IL-6 and TGF-β1 by human monocytes. *Am. J. Reprod. Immunol.* **45,** 205–216
57. Wagner, D. D. (1990) Cell biology of von Willebrand factor. *Annu. Rev. Cell Biol.* **6,** 217–246
58. Dobrkovska, A., Krzensk, U., and Chediak, J. R. (1998) Pharmacokinetics, efficacy and safety of Humate-P in von Willebrand disease. *Haemophilia* **3,** Suppl. 3, 33–39
59. Menache, D., Aronson, D. L., Darr, F., Montgomery, R. R., Gill, J. C., Kessler, C. M., Lusher, J. M., Phatak, P. D., Shapiro, A. D., Thompson, A. R., and White, G. C., 2nd (1996) Pharmacokinetics of von Willebrand factor and factor VIIIC in patients with severe von Willebrand disease (type 3 VWD): estimation of the rate of factor VIIIC synthesis. Cooperative Study Groups. *Br. J. Haematol.* **94,** 740–745
60. Kim, H. J., Kim, P. K., Bae, S. M., Son, H. N., Thoudam, D. S., Kim, J. E., Lee, B. H., Park, R. W., and Kim, I. S. (2009) Transforming growth factor-β-induced protein (TGFBIp/β ig-h3) activates platelets and promotes thrombogenesis. *Blood* **114,** 5206–5215
61. Rees, D. C., Cox, M., and Clegg, J. B. (1995) World distribution of factor V Leiden. *Lancet* **346,** 1133–1134
62. Bertina, R. M., Reitsma, P. H., Rosendaal, F. R., and Vandenbroucke, J. P. (1995) Resistance to activated protein C and factor V Leiden as risk factors for venous thrombosis. *Thromb. Haemost.* **74,** 449–453
63. Bertina, R. M., Koeleman, B. P., Koster, T., Rosendaal, F. R., Dirven, R. J., de Ronde, H., van der Velden, P. A., and Reitsma, P. H. (1994) Mutation in blood coagulation factor V associated with resistance to activated protein C. *Nature* **369,** 64–67
64. Pfaffl, M. W. (2001) A new mathematical model for relative quantification in real time RT-PCR. *Nucleic Acids Res.* **29,** e45
65. Keller, A., Nesvizhskii, A. I., Kolker, E., and Aebersold, R. (2002) Empirical statistical model to estimate the accuracy of peptide identifications made by MS/MS and database search. *Anal. Chem.* **74,** 5383–5392
66. Nesvizhskii, A. I., Keller, A., Kolker, E., and Aebersold, R. (2003) A statistical model for identifying proteins by tandem mass spectrometry. *Anal. Chem.* **75,** 4646–4658
67. Collier, T. S., Sarkar, P., Franck, W. L., Rao, B. M., Dean, R. A., and Muddiman, D. C. (2010) Direct comparison of stable isotope labeling by amino acids in cell culture and spectral counting for quantitative proteomics. *Anal. Chem.* **82,** 8696–8702
68. Collier, T. S., Randall, S. M., Sarkar, P., Rao, B. M., Dean, R. A., and Muddiman, D. C. (2011) Comparison of stable-isotope labeling with amino acids in cell culture and spectral counting for relative quantification of protein expression. *Rapid Commun. Mass Spectrom.* **25,** 2524–2532
69. Fisher, R. A. (1938) in *Statistical Methods for Research Workers* (Crew, F. A. E., and Cutler, W. D., eds) pp. 1–307, Oliver and Boyd, Edinburgh, Scotland, UK
70. Lemmerhirt, H. L., Shavit, J. A., Levy, G. G., Cole, S. M., Long, J. C., and Ginsburg, D. (2006) Enhanced VWF biosynthesis and elevated plasma VWF due to a natural variant in the murine Vwf gene. *Blood* **108,** 3061–3067
71. Mohlke, K. L., Nichols, W. C., Westrick, R. J., Novak, E. K., Cooney, K. A., Swank, R. T., and Ginsburg, D. (1996) A novel modifier gene for plasma von Willebrand factor level maps to distal mouse chromosome 11. *Proc. Natl. Acad. Sci. U.S.A.* **93,** 15352–15357